بسم الله الرحمن الرحيم

Sudan Academy of Sciences (SAS)
Atomic Energy Research Coordination Council

Environmental Geochemistry of ^{238}U, ^{232}Th, ^{40}K and Some Heavy Metals in River Nile Sediments

By:
Saif El Din Mohammed Babiker Siddeeg
B.Sc. Honour (Chemistry)
Faculty of Science, University of Khartoum (2004)

A thesis submitted to Sudan Academy of Sciences in fulfillment of the requirements for the degree of Master of Science in Nuclear Chemistry

Supervisor: Dr. Adam Khatir Sam

June 2007

Environmental Geochemistry of ^{238}U, ^{232}Th, ^{40}K and Some Heavy Metals in River Nile Sediments

By:
Saif El Din Mohammed Babiker Siddeeg

Examination committee

Title	Name	Signature
Supervisor	Dr. Adam Khatir Sam	
External examiner	Dr. Hassan Ibrahim Nimir	
Internal examiner	Dr. Isam Salih Mohamed	

Date of Examination: 11 June 2007

Dedication

To my mother, my father, my sisters and brothers

Acknowledgments

I would like to thank my supervisor Dr. Adam, K. Sam for his support and encouragement throughout my graduate study. I have learned from him great deal about environmental monitoring science and much about scientific discipline. He is definitely my best and most thorough critic.

I particularly like to thank best friend Mr. Alfatih, A. A. Osman, for his contribution in many ways and I appreciate his profound influence to complete this work. I really find him when I face problem and he always there.

My grateful to Prof. M. A. H. Eltyeb the general director of Sudan Atomic Energy Commission (SAEC) for his support to facilitate the measurements of Particle Induced X-ray Emission at Lebanese Atomic Energy Commission.

I'd like to express my appreciation to Lebanese Atomic Energy Commission (LAEC), namely Dr. Nsouli, Dr. Zahraman, Dr. Roumie who gave generously his time to get me started with PIXE technique and helped me to collect and treat PIXE spectra with remarkable efficiency, and Mrs. Lina for her patient through samples preparation for measurement.

I sincerely thank Mr. M. Abdullah and Mr. W. Abdualbagi for their guidance and discussion the results from statistical point of view.

The biggest thanks go to my parents, my sisters and my brothers they reflect to me the beauty in the natural world, appreciate the education so highly, and most importantly giving me emotional support and inspiration, they have made everything possible for me.

Lastly, I thank my friends everywhere and all my colleagues in (SAEC) for encouragements.

ABSTRACT

Environmental geochemistry is concerned with the abundance, distribution, and mobility of chemical elements in surface materials at the surface of earth crust. This study aimed at better understanding of geochemical behavior of U-238, Th-232 and K-40 in river sediments and some heavy elements with emphasis on Mg, Ca, Mn, Fe, Ni, Cu, Zn and Pb. The analysis was conducted for a total of 33 bulk sediment samples from White Nile, Blue Nile and River Nile within Khartoum, the samples were fractionated into seven grain sizes each (2000-1000, 1000-500, 500-250, 250-200, 200-125, 125-100 and < 100 μm), using high resolution gamma-spectrometer for radionuclides measurements, whereas Particle Induced X-ray Emission (PIXE) was used for heavy metals analysis.

On the average, the activity concentration of U-238, Th-232 and K-40 were 17.90±5.23, 16.38±5.34 and 379.82±107.76 Bq kg^{-1} in White Nile, 19.56±5.04, 17.72±4.69, and 494.36±105.79 Bq kg^{-1} in Blue Nile and 19.27±2.88, 17.48±2.78, 359.50±83.15 Bq kg^{-1} in the River Nile sediments. Results revealed inverse relationship between activity concentration and grain size in White and Blue Nile, while the trend is not clear in the River Nile. In general, the variation of the measured values within single grain size was smaller in White Nile compare to Blue and River Nile sediments, and it was observed that the data are highly scattered in grain size (200-125μm). The ratio between U-238/Th-232 is grater than unity in the three rivers indicating that there is relative enrichment of U-238 in the surface sediments. The activity concentration of the fallout radionuclide Cs-137 is one order of magnitude lower in the White Nile sediments (0.89±0.96) Bq kg^{-1} compared to values in the Blue Nile sediments (3.60±1.55) Bq kg^{-1}. Comparison of the values obtained for natural radionuclides and the fallout radionuclide (Cs-137) in the three sites with the global data reflect low and/or insignificant difference.

For heavy metal concentrations, based on the results obtained it was noted that the elements fall into two distinct groups: Mg, Ca, Fe and Mn show high levels and thus they are dominant in the surface sediments, while Ni, Cu, Zn and Pb show low values. The concentrations of the heavy metals reflect no correlation with grain size in the three rivers with the exception of Fe and to some extend Zn.

The plots of heavy metal concentration against the activity concentration of U-238 and Th-232 displayed insignificant positive correlation.

الخلاصة

يهتم عِلم كيمياء الأرض البيئي بوجود وتوزيع و حركة العناصر الكيميائية في الموادِ السطحيّةِ في سطح قشرةِ الأرض. تهدف الدراسة إلي تقديم فهم افصل للسلوك الكيميائي لعناصر اليورانيوم-238 الثوريوم-232 والبوتاسيوم-40 في رسوبيات نهر النيل و رافديه النيل الابيض و النيل الازرق إضافة إلي بعض العناصر الثقيلة مع التركيز علي مجموعة صغيرة تشمل عناصر الماغنزيوم- الكالسيوم- المنجنيز- الحديد- النيكل- النحاس- الزنك و الرصاص.

تم القياس لعدد 33 عينة كلية تم جمعها من ثلاث انهر (النيل الأبيض, النيل الأزرق ونهر النيل) داخل حدود ولاية الخرطوم, فصلت عينات كل نهر علي حده إلي سبعة أحجام حبيبية مختلفة: 1000-2000 , 500- 1000, 250- 500, 200- 250, 125- 200, 100- 125 و اقل من 100 مايكرومتر, تم القياس للنويدات المشعة باستخدام مطيافية غاما عالية الفصل بينما تم قياس العناصر الثقيلة بواسطة مطيافية الجسيمات المستحثة لانبعاث الأشعة السينية.

وجد أن متوسط النشاط الإشعاعي لليورانيوم-238, الثوريوم-232 و البوتاسيوم-40 هو17.90 ±5.23, 16.38 ±5.34 و379.82 ±107.76بيكريل/كيلوجرام في رسوبيات النيل الأبيض, 19.56±5.04, 17.72±4.69 و494.36 ±105.79 بيكريل/كيلو غرام في رسوبيات النيل الأزرق, و19.27 ±2.88, 17.48 ±2.78 و359.50 ±83.15 بيكريل/ كيلوجرام في رسوبيات نهر النيل.

تركيز النشاط الإشعاعي لهذه النويدات المشعة يظهر علاقة عكسية مع الحجم الحبيبي في النيل الأبيض و النيل الأزرق بينما لا تبدو هنالك علاقة واضحة في نهر النيل. من ناحية أخري التباين في القيم التي تم قياسها ضمن الحجم الحبيبي الواحد لهذه العناصر يلاحظ انه صغير ضمن رسوبيات النيل الأبيض مقارنة بالنيل الأزرق و نهر النيل.عموما يلاحظ أن التراكيز أكثر تشتتا ضمن الحجم الحبيبي (125-200) مايكرومتر.

النسبة بين اليورانيوم-238 إلي الثوريوم-232 اكبر بقليل من الواحد في الأنهار الثلاثة مما يشير إلي وجود إثراء نسبي لليورانيوم-238 في هذه الرسوبيات السطحية.

قياس تركيز النشاط الإشعاعي لنويدة السقط النووي السيزيوم-137 يظهر اقل قيمة في رسوبيات النيل الأبيض (0.89 ±0.96) بيكريل/كيلوجرام واعلي قيمة في رسوبيات النيل الأزرق (3.60

±1.55) بيكريل/كيلوجرام, مع ملاحظة إن تركيز هذه النويدة كان اقل من مستوي القياس في كثير من الأحجام الحبيبية لرسوبيات النيل الأبيض.

عند مقارنة تراكيز النشاط الإشعاعي للنويدات الطبيعية و نويدة السقط النووي مع الدراسات المماثلة من البيئات المشابهة نجد أنها إما اقل من أو ضمن نفس مستوي النشاط الإشعاعي لتلك الدراسات.

من قياسات تراكيز المعادن الثقيلة, يمكن تقسيمها إلي مجموعتين اعتمادا علي القيم التي تم الحصول عليها: عناصر الماغنزيوم, الكالسيوم, الحديد و المنجنيز أعطت قيما مرتفعة و تم التعبير عنها بالملي جرام/جرام و تم تصنيفها كعناصر شائعة في الرسوبيات السطحية في منطقة الدراسة, و عناصر النيكل, النخاس, الزنك و الرصاص التي أعطت قيما منخفضة وتم التعبير عنها بالمايكروجرام/جرام.

تراكيز العناصر الثقيلة تظهر عدم وجود علاقة بين التركيز والحجم الحبيبي في رسوبيات الانهارالثلاثة عدا الحديد و إلي حد ما الزنك.

أظهرت المعادنُ الثقيلةُ ارتباط إيجابيُ غير معنوي مَع النويدات الطبيعية (اليورانيوم -238 و الثوريوم -232).

TABLE OF CONTENTS

List of Tables

List of Figures

Chapter One

Introduction

Environmental geochemistry is a complex topic, and it is as a multi-disciplinary science, it draws on the fields of geology, chemistry, and biology to provide information essential to environmental management, planning, and health protection. Metals in the rivers originate from natural as well as artificial sources. Metals that are naturally introduced into the river come primarily from such sources as rock weathering, soil erosion, or the dissolution of water-soluble salts. Naturally occurring metals move through aquatic environments independently of human activities, usually without any detrimental effects.

Sediment is a matrix of materials which is comprised of detrital, inorganic, or organic particles, and is relatively heterogeneous in terms of its physical, chemical, and biological characteristics. Hakanson, (1992) stated that sediments have a marked ability for converting inputs of metals from various sources into sparingly soluble forms, either through precipitation as oxides or carbonates, or through formation of solid solutions with other minerals. Thus, aquatic sediments constitute the most important reservoir or sink of metals and other pollutants. As the particle size influence very much the properties of dispersed system especially sediments, there is a relationship between the particle size and the chemical and geochemical of radionuclides and heavy metals in the aquatic system include sediments. The particle size is determined by dry sieving to the sediments. However, as the valleys of the River Nile and its tributaries were settled and industrialized in some locations along its flow, the metals added by human activities have affected the water quality of the river, so studying the speciation of these elements in aquatic system is important.

Global estimates of sediment transport in major rivers of the world vary widely, reflecting the difficulty in obtaining reliable values for sediment concentration and discharge in many countries. So having radioactivity maps can provide an advantage highly useful for environmental studies and geological mapping often indicating features not seen by other techniques. Radiation, specifically gamma rays, is released through the spontaneous decay of radioactive elements. The three most common naturally occurring

radioactive elements are potassium, uranium and thorium; these elements are found at some concentrations in most rock-forming minerals. Potassium, for example, occurs mainly in the mineral feldspar which is an abundant and widespread mineral in the earth's crust, and a prominent component of granitic rock. Uranium and thorium are generally present in low concentrations (measured in parts per million (ppm)) in a wide range of minerals, where uranium occurs at high concentrations, it represents a target of economic interest to mining companies.

From environmental surveys, using the distinctive gamma-ray spectra from potassium and the daughters of the two radioactive elements; uranium and thorium, high resolution gamma-ray spectrometry used to measure the activity concentrations of K-40, U-238, Th-232 and the fallout radionuclide Cs-137 which can be used to compose the radiation map of the country addition to know their geochemistry in different grain size of surface sediments. Although, there is an increasing awareness of the hazards that exist due to the contamination of fresh water produced from industry, little is known about the concentration of heavy metal in River Nile sediments, whereas no data about their behavior and association in different component of aquatic system. In this study and in order to give a complete image from environmental geochemistry point of view, Particle Induced X-ray Emission (PIXE), with it's high sensitivity and multi-elemental capability and which has been proved to be a very useful technique for obtaining the concentration of heavy elements in aquatic sediment, used to investigate the associate of heavy metals in different grain sizes of sediments, these elements include: magnesium, calcium, manganese, iron, nickel, copper, zinc and lead.

1.1 Environmental Geochemistry of Uranium and Thorium

1.1.1 Geochemical associations

Natural radionuclides from uranium and thorium series are present everywhere in the environment. They are part of soil, rocks, water, and food and can also be detected in the human body. Uranium-238 and thorium-232 are parents of two complex series of radioactive elements, with lead being the last (stable) element in both series. The uranium normally found in nature consists of three isotopes having mass number 234, 235 and 238. In the earth's crust ^{238}U is present in the amount of 99.28%, and is usually in

radioactive equilibrium or near equilibrium with its daughter ^{234}U. Thorium normally found in nature consists of three isotopes having mass number 232 and 228, in ^{232}Th decay-series, and 230 in ^{238}U decay-series. Uranium and thorium are present in the earth's crust at average concentrations of 4.2 and 12.5 ppm, respectively (Shawky *et al.*, 2001). The constancy of this value in many different igneous rocks indicates the general lack of fractionation of the two elements during magmatic processes. Uranium and thorium are preferentially incorporated into late crystallizing magmas and residual solutions, because their large ionic radii preclude them from early crystallizing silicate. Therefore, they are found associated mainly with granite and pegmatite. The geochemistry of uranium and its deposits has been studied intensively because of the importance of this element as a source of energy based on industrial fission of ^{235}U. Thorium is now thought to be about three times as abundant as uranium (UNSCEAR, 1993). In addition to its importance as a nuclear fuel, thorium is widely used in industry. Uranium and thorium and their compounds are highly toxic from both chemical and radiological standpoints. Exposure to thorium and uranium is encountered in the mining and milling of elemental ore materials and at various other stages in the elements industry. Uranium-238 and thorium-232 are primordial radionuclides. In most places on earth they vary only within narrow limits, but in some locations there are wide deviations from normal levels.

1.1.2 Effect of weathering

In the oxidizing zones of terrestrial near-surface environment, both uranium and thorium mobilized, but in different ways. Thorium is largely transported in insoluble resistant materials or is adsorbed on the surface of clay minerals. In the other hand, uranium may either move in solutions as a complex ion, or like thorium, in adsorbed or detrital phase. Both elements occur in +4 oxidation state in primary igneous rocks and minerals, but in near surface environment, uranium may oxidize to (V) and (VI) states.

In the (VI) state uranium forms soluble uranyl complexes ions (UO_2^{+2}) which play the most important role in uranium transport during weathering. If a geological formation containing ^{238}U and ^{232}Th is left undisturbed for very long periods of time, the members of the individual decay series will grow, reaching a state of ‘‘secular equilibrium’’ which

is characterized by the fact that every element in the series will present the same activity. This is not the case, however, if one of the radionuclides (like ^{226}Ra) migrates in the soil matrix and is deposited somewhere else. If this condition occurs, the equilibrium is disrupted and the secular equilibrium will not exist anymore. This radium is then said to be ‘‘unsupported’’, meaning that its activity is not related to the activities of its predecessors in the series and thus "Radioactive disequilibrium" is induced between the nuclide above and bellow radium. At the same manner radon gas may be a reason of such disequilibrium since it can diffuse out of a deposit if the structure is slightly porous.
Uranium is a redox-sensitive and biologically-related element, and a small change to more reducing conditions may immobilize the soluble U (VI) to insoluble U (IV), while more oxidizing conditions have the reverse effect. Transfer of uranium from water to sediments is known to arise from adsorption and/or adhesion onto settling particles including organic matter. Additional transfer of uranium may result from diffusion into the sediments and reduction of U (VI) to U (IV) with precipitation of U $(OH)_4$ at the redox boundary. Thorium is an element mostly associated with terrestrial materials, and is well known as an immobile element. Thorium has an extremely low solubility in water and is conserved during chemical weathering processes. Therefore, thorium is recognized as a proxy for terrestrial materials. Lake bottom sediments contain uranium and thorium isotopes originating mainly from two sources: one is U (Th) fraction in soil itself derived from river and direct discharge (hereafter referred to as terrigenous U (Th)) and the other is U (Th) fractions which is formed mainly from a dissolved phase within the lake and its input rivers (hereafter referred to as authigenic U (Th)). Actually, the authigenic (U) in sediments seems to reflect the physico-chemical conditions of sedimentation and environmental changes and thus it is essential to separate the two uranium sources.

1.1.3 Sources of uranium and thorium

1.1.3.1 Igneous rocks

Uranium and thorium are highly concentrated in continental igneous rocks and in particular, silicic rocks such as granite are enriched with uranium and thorium up to two orders of magnitude over oceanic basalts. There are three ways in which uranium and thorium can distributed in igneous rocks: by direct cation substitution in the silicate of the

major rock forming minerals; as minor or major component of accessory minerals such as monazite and zircon; and by adsorption in lattice defects or onto crystal and grain boundaries (Ivanovich, 1992).

1.1.3.2 Sedimentary and metasedimentary rocks

Most clastic sediments contain uranium level in the range of 0.5-4 ppm, while organic-rich shales and marine phosphates contain uranium in the level of 3-1200 ppm. Thorium concentration in most clastic sediments is similar to the sources rock and this refer to low solubility of thorium in natural waters, while mostly due to mechanical sorting process, high thorium concentration found in some sands.

1.1.3.3 Recent sediments

Certain organic sediments such as humic substances are enriched in uranium and they play important role in adsorption of uranium and thorium from water (Zielinski and Meier, 1988). Thorium content of recent authigenic sediments is generally low. Degnes *et al*., (1977) studied uranium in Black Sea mud's and thought that living organic material , such as plankton, is also be capable of complexing uranium, and this supported from Mann and Fyfe (1985) by showing that the concentration of uranium is in order of 10^3 to 10^5 over in fresh–green algae than surrounding river water. Reduction of uranium from hexavalent to tetravalent state occur after complexing either by H_2S produced from the decomposition of organics, (Langmair, 1978), and this known as sulphate-reducing organism (Lovley and Philips, 1992).

$$4(UO_2\,(CO_3)_3^{-4} + HS^- + 15H^+ \rightarrow \quad 4UO_2 \quad + SO_4^{2-} + 12CO_2 + 8H_2O$$

The other way of reduction U^{+6} to U^{+4} is by iron reducing (Fredrickson *et al*., 2000).

1.1.3.4 The hydrosphere

Uranium content in fresh water varies from 0.01 to 5 ppm in surface waters, and from 0.1 to 50 ppm in ground waters (Gascoyne, 1992). This refers to the variability associated with fresh waters, which depend on factors include: contact time with the uranium–bearing horizon, uranium content of the horizon, and amount of evaporation and availability of complexing ions. The content of thorium in natural waters is extremely low, Moore (1981) determined ^{232}Th content of surface and deep-sea waters and found it

is about 0.01 to 0.03 dpm.ton^{-1} (0.027 ng.Kg^{-1}) and ^{230}Th is 0.03 to 0.13 dpm.ton^{-1} and 0.3 to 2.7 dpm.ton^{-1} in surface and deep-sea waters respectively.

1.1.3.5 Ore deposits

The study of ore deposits of uranium and thorium provide much information about their geochemistry, these economic sources of uranium, which are thought to have been formed by precipitation from hydrothermal solutions or ground waters in reducing environment, contain uranous oxides; uraninite (UO_2), pitchblende (UO_2 to UO_8), silicate and coffinite($USiO_4$). The whole amount of environmental uranium is almost uniformly dispersed in nature. In surface soils, its concentration ranges from 0.1 to 20 mg kg^{-1} with a world average value of 2.8 mg kg^{-1} (UNSCEAR 2000a, b). The most economic sources of thorium is monazite ((Ce, Y, La, Th) PO_4), because of its frequent occurrence as placer deposits in detrital sands. The silicates, thorite, ($ThSiO_4$), and oxides thorianite (ThO_2) are also sources of thorium (Ivanovich, 1992).

1.1.4 Geochemical cycles

1.1.4.1 Mobilization and transport in solution

Uranium and thorium in tetravalent oxidation state are both immobile in near surface environment at low temperature, but due to the probability of uranium to oxidize to hexavalent state, uranium is relatively soluble and may mobilize (langmuir, 1978).

$$U^{4+} + 2H_2O \rightarrow \ UO_2^{2+} \ + 4H^+ \ + \ 2e^- \qquad E_0 = 0.27 \text{ V}$$

Uranium solubility in aqueous system is predominantly controlled by three factors; oxidation–reduction potential, pH, and dissolved carbonate (Murphy and Shock, 1999). Osmond and Cowart (1992) reviewed that; under reducing conditions, uranium (IV) complexes with hydroxide and fluoride are only the dissolved species in natural waters, and the precipitation of U^{4+} is the dominant process leading to naturally enriched zones of uranium in the subsurface. Higher disequilibrium has been noticed rather in the seawater than in the sediments. Ku *et al*. (1977) reported that, the ^{234}U/^{238}U activity ratio in the majority of natural waters equals 1–2, but in groundwater it ranges between 0.52 and 9.02. Also surplus of ^{234}U is in seawater, but the ^{234}U/^{238}U activity ratio in seawater (especially in oceanic water) is relatively constant and equals 1.14. The ^{234}U/^{238}U in

saline waters (brines) is between 1.11 and 5.14 (Baar *et al*., 1979). Bottom waters (main component of brines) probably have an effect on radioactivity disequilibrium between isotopes of uranium. In river waters the values of the $^{234}U/^{238}U$ activity ratio are between 1.00 and 2.14, but for the majority of the rivers it is equal to 1.20–1.30 (Miyake *et al*., 1973). If the reduction process from U (VI) to U (IV) was dominant in reduction areas of the Southern Baltic, we can expect the same value of the $^{234}U/^{238}U$ activity ratio in sediments and bottom water and these values should oscillate near 1.17. In this case the major contribution of uranium to sediments is by uptake from the water column (Skwarzec *et al*., 2002). The reduction of Uranium from (6^+) to (4^+) can be microbially mediated, and the geomicrobiology of uranium was reviewed by Suzuki and Banfield (1999). In oxidizing aqueous environment, Uranium (VI) complexes are more soluble than uranous species , and uranium (VI) is present as the linear uranyl dioxo ions (UO_2^{2+}) and an array of mononuclear and polynuclear hydroxide species. Mononuclear uranyl carbonate species become more important with increasing carbonate concentrations (Girmmar, 2001).

1.1.4.2 Mobilization and transport in particulate matter

Clearly the association of uranium and thorium with solid phase and the mobility of them depend on the site-specific conditions. Unless chemical interactions occur across the phase boundary, the movement of uranium and thorium as particulate matter is controlled only by physical properties and flow velocity of the transporting medium. Thorium is predominant transported in particulate matter and this refers to its extremely low solubility in most natural waters. Even when thorium is generated in solution by radioactive decay of uranium, it rapidly hydrolyses and adsorbs onto the nearest solid surface. For this reason, the upper layers of deep-sea sediments are found to contain high activities of unsupported ^{230}Th and the $^{230}Th/^{234}U$ activity ratio of ocean waters is less than 0.01 (Ku, 1976). The ocean water origin of this excess of ^{230}Th is further demonstrated by the high activity ratio of $^{230}Th/^{232}Th$ (up to 158) of recent pelagic clays in the South Pacific Ocean.

1.1.5 Depositional process in the near surface environment

1.1.5.1 Inorganic and biogenic precipitation

In solutions, when uranium present as carbonate species, reduction of partial pressure of carbon dioxide by degassing to the atmosphere will case precipitation of uranium with another mineral as coprecipitation.

1.1.5.2 Adsorption

Insoluble hydroxides and oxides and clay minerals are removed from solution by adsorption onto the surface of detrital particulates (inorganic and organic), these nuclides produced from radioactive decay of uranium in sea water either from hydrolyzates or adsorb directly onto particulate before descending to the ocean floor.

Removal of uranium from solutions in fresh waters and anoxic ocean-bottom waters occur by reduction to the less soluble U^{4+} species. There are two ways in which the deposition of uranium occur with organic materials; either directly by surface adsorption of U^{4+}, or indirectly by precipitation of insoluble uranyl compound followed eventually by reduction.

1.1.5.3 Sedimentation

The transportation of un-weathered detrital minerals of uranium and thorium from continental areas by rivers and tidal current is the main process via which uranium and thorium enter lakes, estuaries and continental shelf environment. In tropical areas, where the rate of erosion is high, mechanical sorting of sediments increase the concentration of heavy resistant minerals such as monazite and zircon in sands of beach. The terrigenous clays in deep waters are diluted with biogenic sediments , and these deposits are contain uranium series nuclides in amount determined by their concentration in sea water, biological fractionation mechanism, and the rate of descent through water column after death, in the same time these deposits are depleted in detrital thorium (Ivanocich, 1992).

1.2 Heavy Metals in Aquatic System

Occurrence of heavy metals in surface water system can be originated from natural or anthropogenic sources. The natural processing cause the cycle of heavy metals in the

environment and this supported by the man's activity. Under normal conditions, river appear as the most important source of heavy metals in the aquatic system, this refer that the river water contain mechanical and chemical weathering products of rocks, either in solutions or particulates or sediments, addition to the compounds washed during the rain fall from the atmosphere and originally have been contained in salt particles from the land (Idris, 1999). Sediment is a matrix of materials which is comprised of detrital, inorganic, or organic particles, and is relatively heterogeneous in terms of its physical, chemical, and biological characteristics.

Sediments as sinks for heavy metals, thus they become more or less important part of ecosystem. Many conditions such as pH, redox-potential, ionic strength and the concentration of organic complexing agents affecting directly the release of heavy metals into the water phase, so sediments also consider as a source of heavy metals (Saenz *et al*., 2003).

The second important source of heavy metals is man-made sources, which include chemical, metal industries and most of industrial processes involving water. The discharge of this waste in aqueous system leading to enrichment of the concentration of elements in water. Idris (1999) mentioned the major sources of anthropogenic pollutions, and these include: industrial manufacturing processes, domestic waste-water usually contains elements such as lead, zinc and copper, electrical power plants as a result of burning of coal and oil, industrial metal processing which represents the main pollutant are nickel and chromium, tanning industry from which chromium is released as a major pollutant, fertilizers production (cadmium as by-product), paper manufacturing releases mercury as major element in the effluent and the atmosphere fallout in which lead is considered as the main element.

1.2.1 Speciation of heavy metals in aquatic sediments

The physical and chemical form in which the particular element is found is the simple meaning of the term speciation. Aquatic sediments play a role of historical record for accumulation of heavy metals addition to indication of pollution in the aquatic system. In sediments, heavy metals can be present in various chemical forms, and generally exhibit different physical and chemical behaviors in terms of chemical interactions, mobility,

biological availability and potential toxicity. It is necessary to identify and quantify the forms in which a metal is present in sediment to gain more precise understanding of the potential and actual impacts of elevated levels of metals in sediment, and to evaluate processes of transport, deposition and release under changing environmental conditions. A lot of investigations of the behavior of individual heavy metals in aquatic sediments were done by many researchers, the aqueous chemistry of copper has been studied (Mantoura *et al*., 1978), and they found about 90% of Cu in river water was complexed by dissolved humic matter. In the absence of organic ligands, the most important processes explain the chemistry of Cu^{+2} are hydrolysis and precipitation of copper hydroxide and carbonate in aerated waters. Adsorption onto suspended matter and sediment is the major behavior of lead in fresh and saline water; although lead is differ from copper behavior in organic matter (Mance *et al*., 1984). The main complexes of lead in river water are carbonate in pH 7-9 and hydroxide. The concentration of lead in sediment is higher in compare to water according to its solubility (Rudd *et al*., 1984). Nickel speciation considered in both soluble and particulate matter, and about 90% of nickel in an aerated fresh water is constitute of ionic nickel compare to the complexation with natural ligands. In general nickel tend to form weak complexes with organic ligands and the portion of total nickel associated with particulate vary from 7-99% reflecting the variation in source rock and effect of industrialization (Rudd *et al*., 1984). In aerobic water like fresh water, a significant amount of zinc is like to exit in ionic form such as carbonate, hydrated ions and stable organic compounds addition to adsorption in organic and inorganic collides (e.g. hunmic), and the later increase significantly when the pH above 7 (Idris, 1999).

Any individual element seems to has its own behavior in aquatic environment, but in general under normal environmental conditions, it appears that Cu, Ni and Pb would associate with suspended particulate matter (60-80 %) while Zn and Cd like to remain in solutions (30-40 %)

1.2.2 Association of heavy metals with different grain size of sediments

Korede *et al*. (2005) reported that there are two components composed the surface sediments; 1) mineral originate from bedrock erosion; and 2) organic component arising during soil-formation processes, and the later include biological and microbiological

production and decomposition. Classification of sediments depends on many factors, one of them is the form in which sediment particles found, in the case of suspended matter sediment particles transfer with water current because they found in water column, whereas in deposited sediments the particles found in the bed of lake or river.

One of the most important factors that influence ecological health is the surface sediment size distribution, and considering this Hakanson and Jansson (1983) classified sediments to the following categories; $\leq$ 2mm (sand fraction), $\leq$ 63μm (silt fraction) and $\leq$ 2μm (clay fraction). This distribution affects surface sediment stability and sediment transport rates by defining the roughness of the river.

The role of sediment in chemical pollution is tied both to the particle size of sediment, and to the amount of particulate organic carbon associated with the sediment. The chemically active fraction of sediment is usually cited as that portion which is smaller than 63 μm (silt + clay) fraction. Many heavy metals (including radionuclides) and toxic materials are transported through streams by binding to fine sediments, and for heavy metals particle size is of primary importance due to the large surface area of very small particles. The concentration of trace elements on stream bed materials is strongly affected by the particle-size distribution of the sample (Rickert *et al*., 1977; Wilber and Hunter, 1979). Generally, the concentration of trace elements on stream bed materials increases as particle size decreases. Heavy metals tend to be highly attracted to ionic exchange sites that are associated with clay particles and with the iron and manganese coatings that commonly occur on these small particles. Organic matter content strongly associated with sediment and transported as part of the sediment load in rivers, so its play an essential role in the high concentration of heavy metals in sediment addition to surface area of fine grain size, and this importance appear clearly in case of high concentration of heavy metals in coarse sand (Osman, 2006).

1.3 Objectives of the Research

This study is aimed at:

a. Building base-line data on the activity concentration of uranium, thorium, potassium, caesium and the concentration of some heavy metals in River surface sediments.

b. Better understanding of the nature of distribution of primordial radionuclides and heavy metals in River deposits.
c. Characterizing the geochemical aspects as to which sediments size fraction the uranium, thorium, potassium and some heavy metals are associated with.
d. Exploiting the produced data as a blue-print for possible understanding the nature of sedimentation processes in dynamic system such as River Nile and its main tributaries.

Chapter Two

Literature Review

The study of radioactivity and pollution in surface river sediments as one topic is rarely published worldwide. In fact, there is lack of information in the fields of environmental geochemistry and radioactivity in River Nile or its tributaries (White and Blue Niles) in Sudan, in spite of Sudan is the only country contains the great Nile and most of its tributaries. However, a similar work has been initiated by Sam *et al*. (1998a, 1998b, 2000a) and continued under his supervision in most cases to build up base line data of radioactivity in the whole country.

Sam *et al*. (1998a) investigated the distribution of some natural and anthropogenic radionuclides (^{226}Ra, ^{228}Ra, ^{40}K and ^{137}Cs) in surface marine sediments from the harbour of Port Sudan and Sawakin on the Sudanese coast of the Red Sea, using direct high-resolution γ-spectrometry. Evaluation of the results showed that there is no enhancement by anthropogenic from hinterland. The average activity concentration of ^{226}Ra, ^{228}Ra, ^{40}K and ^{137}Cs in Port Sudan harbour sediments were 11.05, 10.35, 311 and 7.02 Bq Kg^{-1} respectively, whereas in Sawakin harbour sediments were 12.61, 6.18, 192 and 4.51 Bq Kg^{-1} respectively.

Measurement of natural and fallout radionuclides in different environmental samples, including sediments, from the Sudanese coast of the Red Sea have been made by Sam *et al*. (1998b). Activity concentration level of uranium isotopes, thorium isotopes, ^{226}Ra, ^{40}K, ^{137}Cs and other radionuclides were determined in the samples and the average values were 29.6±16.3, 11.6±15.2, 6.6±4.6, 6±6.1, 48.4±20.9 and 158.4±161.9 Bq Kg^{-1} for ^{238}U, ^{226}Ra, ^{230}Th, ^{232}Th, ^{228}Th and ^{40}K respectively. The obvious conclusion was that the activity concentration of the Red Sea is similar to the average activity of each of radionuclides from other areas around the world.

Michihiro *et al*. (1987) investigated the concentrations of the three nuclides in river-bed soil from the upstream area of Yoshii-River in Okayama Prefecture (Japan), samples were sieved into six fractions according to particle-size and the concentrations of the three nuclides were measured, they investigated that the activity concentration increased

with decrease in particle-size of soil on all samples, though the particle-size distributions varied with both sampling location and date. Thus the concentration of each nuclide in a fine river-bed soil was found to show effectively the latest level of pollution in the river water. The concentrations of ^{238}U in each fraction of the two samples were measured by gamma-ray spectrometer with intrinsic Ge-detector and ^{226}Ra also with Ge (Li) detector. The concentrations of both nuclides adsorbed on the soil and the $^{226}Ra/\ ^{238}U$ ratio were estimated with respect to the specific surface-area in each fraction.

Alam *et al*. (1997) have analyzed sediment samples from the Karnaphuli river estuary, near shore, and off-shore regions of the coast of Chittagong in the Bay of Bengal for their natural radioactivity contents of ^{232}Th, ^{238}U and ^{40}K and anthropogenic radioactivity contents of ^{137}Cs and HPGe gamma spectrometry, together with the measurement of sediment pH and grain size analyses of the collected samples. The activity concentration found in sediment ranged from 10.44 ± 2.31 to 64.02 ± 8.13 Bq kg^{-1} for ^{232}Th, 5.87 ± 1.21 to 27.85 ± 1.71 Bq kg^{-1} for ^{238}U, l18.28 ± 19.70 to 608.21 ± 75.70 Bq kg^{-1} for ^{40}K, and 0.09 ± 0.06 to 4.64 ± 0.19 Bq kg^{-1} for ^{137}Cs.

Selected sedimentary samples were collected from different locations on the east and west banks of the River Nile in Upper Egypt for natural radioactivity measurements to detect the presence of radioactive elements. From the analysis of radiations from ^{226}Ra, ^{232}Th and ^{40}K isotopes, the samples were found to contain ^{226}Ra, ^{232}Th and ^{40}K in concentrations up to 52 ± 7.3, 76.2 ± 6.2 and 351.9 ± 17.6 Bq kg^{-1}, respectively (Uosif, 2006).

Akram *et al*. (2006a) reported natural radionuclide contents of ^{226}Ra, ^{228}Ra and ^{40}K for inter-tidal sediments collected from selected locations a long Balochistan Coast using HPGe detector based gamma-spectrometry system. The sampling zone extends from the beaches of Sonmiani (near Karachi metropolis) through Jiwani (close to the border of Iran). The natural radioactivity levels detected in various sediment samples range from 14.4 ± 2.5 to 36.6 ± 3.8 Bq $kg^{-1}$for ^{226}Ra, 9.8 ± 1.2 to 35.2 ± 2.0 Bq kg^{-1} for ^{228}Ra and 144.6 ± 9.4 to 610.5 ± 23.9 Bq kg^{-1} for ^{40}K, no artificial radionuclide was detected in any of the marine coastal sediment samples. ^{137}Cs contents in sediment samples were below the limit of detection.

Akram *et al*. (2006b) reviewed activity concentration of gamma emitting radionuclides in shallow marine sediments of the Sindh coast using a gamma spectrometry technique. The activity concentration has been found to vary from 15.93 ± 5.22 to 30.53 ± 4.70 Bq kg^{-1} for ^{226}Ra, from 11.72 ± 1.22 to 33.94 ±1.86 9.8 ± 1.2 to 35.2 ± 2.08 Bq kg^{-1} for ^{228}Ra and from 295.22 ± 32.83 to 748.47 ± 28.75 144.6 ± 9.4 to 610.5 ± 23.9 Bq $kg^{-1}$for ^{40}K. No artificial radionuclide was detected in the samples measured from the study area. As no data on radioactivity of the coastal environment of Pakistan are available, the data presented here will serve as baseline information on radionuclides concentration in shallow sea sediments of the Sindh coast.

Sediment samples from the coast of Kuwait were studied and the activity concentrations of natural as well as man-made radioactive sources were measured using Gamma-ray spectrometry. The coast of Kuwait is mainly soft sedimentary colitic limestones or sandstones, overlaid in many areas with beach or wind-blown sand. In the north, suspended material from the Shatt Al-Arab delta has settled to form extensive soft areas of inter tidal mud within Kuwait Bay. The radioactivity in southern areas reaches about one half of the values commonly assigned as the world average. In the northern areas, higher radioactivity concentrations are found but are still below the international levels (Saad and Al-Azmi, 2002).

The natural radioactivity levels in sediments collected around Ikogosi warm spring, Nigeria, has been determined using a highly sensitive HPGe detector. The mean activity concentration of ^{40}K, ^{226}Ra and ^{228}Ac were measured and found as followed 113.89 ± 5.64, 21.47 ± 5.14 and14.20 ±1.07 Bq kg^{-1} for ^{40}K, ^{226}Ra and ^{228}Ac respectively (Isinkaye and Ajayi, 2006).

Surface sediments measurements according to grain size for heavy metals as well as radioactivity were conducted by Idris (1999) in Sudanese coast of the Red Sea. Five fractions were analyzed for Mn, Fe, Ni, Cu, Zn and Pb; the range of concentration were 53.3-819μg/g, 1.4-51 mg/g, 8-131 μg/g, 9.5-113 μg/g, 18.4-142 μg/g, and 4-26.6 μg/g respectively. From heavy metals measurement, it's appear that for some samples there was increasing of concentration with decreasing of particle size supporting the meaning of anthropogenic contribution to these samples. For activity concentration the values were 2.2-25.1 Bq kg^{-1} (^{226}Ra), 2.1-13.1 Bq kg^{-1} (^{228}Ra), 21.6-429 Bq kg^{-1} (^{40}K) while

^{137}Cs was found below detection limits in most measurements and 8.3 Bq/Kg was the highest value for it.

Sir El Khatim (2002) presented data of some natural and artificial radionuclides as well as trace elements in marine environment. Surface sediments samples from shallow water were analyzed and the activity concentration of ^{238}U, ^{234}Th and ^{40}K were 2.14-6.69, 27.3-79.4 and 462-656 Bq kg^{-1} respectively, whereas ^{137}Cs was not detected in all samples. Concentration of trace elements was 0.8-20.5 ppm, 1.9-39.3 ppm, 6.3 ppm and 2.23 ppm for Pb, Cr, Zn and Ni respectively. The conclusion of these values indicated that the surface sediments from these coastal are poor in both radioactivity and trace elements measurements compared to the global data available.

The pollution of Mooi River in South Africa has been reported after determination of some heavy metals in sediment of the river. The study concerning with Cd, Pb, Cu and Zn. Concentration of cadmium was found in the clay fraction in the range 66-107 μg/g, and for lead it was 34-62 μg/g, zinc concentration was 25-59 μg/g while copper concentration was found higher than the global data, and it was in the range of 11-36 μg/g (Van Aardt and Erdmann, 2004).

Evaluation of the contamination in Suzhou River in China was done by Yuanxun *et al*. (2003) using PIXE technique for determination the concentration of some heavy elements such as Cr, Mn, Fe, Zn and Pb. The results demonstrated that the elemental content of these heavy metals in the river gradually decreased with the rising tide. Minimum concentration observed at high tide and the maximum were in the ebb tide.

Silt-sandy bottom sediments of the Odra River were studied (standard < 2 mm fraction, of diversified grain-size distribution). The heavy metals content was determined in various grain-size sub-fractions [mm]: < 0.2, < 0.1, < 0.06 and < 0.02. Samples contain variable amounts of Cd, Co, Cr, Cu, Fe, Mn, Ni, Pb and Zn. Heavy metals concentrations increase with the decreasing grain size. In general, fractions < 0.02 mm contain from 7.7 (Co) to 19.0 (Cu) times more metals than the raw sediments, while in case of fractions < 0.2 mm metals content exceeds 5.7 (Co) to 14.5 (Cu) times content in the raw sediments. Finer fraction collects from 23% (Co) to 44% (Cu) of overall metal amount in the raw sediment whereas coarser one concentrates from 44% (Co) to 70% (Cu). The linear correlation between metal concentration in the raw sediment and contents of the

particular grain-size fractions has been found. Similarly, a linear correlation was also found between metal concentrations in the raw sediment and contributions of metals in each fraction to the raw sediments. (Aleksander *et al*., 2003)

The distribution of Si, Al, Fe, Mn, Cu, Zn, Ni and Cr in different grain-size fractions and geochemical association of Fe, Mn, Cu and Zn with <63-μm size fraction of bed sediments of Damodar River has been studied. In general, concentrations of heavy metals tend to increase as the size fractions get finer. However at two sites, near mining areas, the coarser particles show similar or even higher heavy metal concentrations than finer ones. The higher residence time and/or presence of coarser particles from mining wastes are possibly responsible for higher metal content in the coarser size fractions. The chemical fractionation study shows that lithogenic is the major chemical phase for heavy metals. Fe and Mn are the major elements of the lithogenic lattice, constituting 34-63% and 22-59%, respectively, of total concentrations. Fe-Mn oxide and organic bound fractions are significant phases in the non-lithogenic fraction. The carbonate fraction is less significant for heavy metal scavenging in the present environment and shows the following order of abundance Zn>Cu>Mn>Fe. The exchangeable fraction of the Damodar sediments contains very low amounts of heavy metals suggesting poor bioavailability of metals (Singh *et al*., 1999).

John *et al*. (1989) studied the concentration of some heavy metals in sediments samples collect from the Ohio River, and they found that the concentration of metals generally decreased with distance downstream, with highest values occurring in the industrial areas along the river.

Chapter Three

Experimental Techniques

3.1 Introduction

Spectroscopic methods are the widely applied techniques for elemental analysis in sediments, and this refer to their accuracy, good precision and high sensitivity. There are many factors determine the appropriate technique for elemental analysis, but expected concentration of the elements of interest in the sample play essential role among other factors. For measuring radioactivity and heavy metals, there are several techniques called Nuclear Analytical Techniques using for this purpose, from which we consider in this study with gamma-ray spectroscopy to determine the activity concentration of natural occurring radionuclides: ^{238}U, ^{232}Th, and ^{40}K and anthropogenic nuclide ^{137}Cs, whereas particle induced x-ray emission (PIXE) was used to determine heavy metals in the samples, namely magnesium, calcium, manganese, iron, nickel, copper, zinc and lead.

There are four major essential components required in any simple electronic system used in nuclear radiation detection as shown in Fig. (3.1).

The main aspect in the detection of nuclear radiation depends on the interaction between the radiation and the detector, which end with giving all or some energy of the incident radiation to the detector medium, either by direct ionization or by emission of a charge particle which produces ionization in the detector medium. Several methods are applied to detect this ionization; either by direct collection of produced charge by electrical mean as in semiconductor detectors, or by emission of photons as in scintillation detectors. The amplification system consist from preamplifier and the amplifier is used to amplify and shape the pluses whose amplitudes are proportion to the energy of detected radiation before send them to a pulse height analyzer, which sort the pulses according to their amplitudes leading to form the required spectrum. The digital signal which proportional to the pulse height made in analog-to-digital converter after the pulse inter in it, then sorting of the signal into channels or memory to output the spectrum data is the final step of process.

3.2 Gamma spectrometry

Gamma-ray spectroscopy using the method of pulse height analysis makes possibility of detecting gamma-emitters in the original sample without chemical separation. Such determinations, as in alpha- and beta-spectroscopy, are possible because the method provide a basis for the identification of specific nuclear transitions, which in turn characteristic on specific radionuclides. Thus, both qualitative identification and quantitative determination of radionuclides in the sample can be done using this technique. The obvious advantages of gamma-ray spectrometry refer to the fact that gamma-radiation is much greater penetration compared with alpha and beta-particles, and hence; the method is non-destructive, sample preparation is straightforward and many nuclides can be analyzed simultaneously including natural and anthropogenic. The form in which the sample is presented to gamma-ray detectors depend on many factors such as; the type of the sample, the available equipment, the composition of radionuclides and the level of activity. The standard containers that are widely used are Marinelli beakers and aluminium cans. Measuring time varies according to the sample type, required detection limits, detection efficiency and radionuclides of interest. Detection of gamma-rays is carried out either by semiconductor detectors in which conduction is activated by the energy given from gamma photons, or by scintillation detectors (organic crystal), where gamma photons are detected by photomultipliers. Semiconductor detectors have high-resolution, this means good discrimination between most emissions lines, and therefore used for direct quantitative spectrometry on complex samples like environmental samples. There are several geometries of detectors available, all are based on a high-purity germanium detectors cooled close to the temperature of liquid nitrogen (77K) to give best possible resolution by minimizing leakage current of the detector, and those are planner, closed-end coaxial and well type detectors. Inorganic scintillation detectors, on the other hand, have poor resolution and for this they use mainly confined to total activity measurements or to spectrometry aimed at determining a limited number of radioisotopes and therefore for samples which have received preliminary chemical separation.

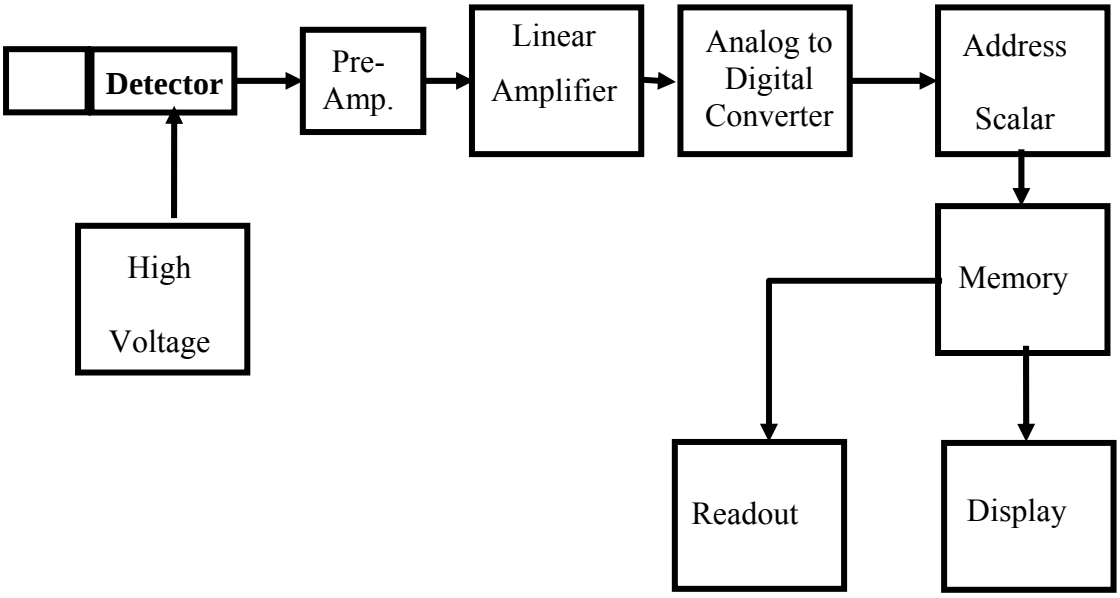

Fig. 3.1: The general component of electronic system in nuclear instrumentation

3.2.1 Calibration

To allow for reliable calibration, samples must be presented to the detector in a reproducible geometry, and should be sealed good enough to provide maximum sensitivity in the analysis of uranium and thorium via short-lived daughters of radon gas, (Ivanovich, 1992). To achieve identification and quantification measurements on unknown radionuclides, gamma spectrometer was calibrated with respect to energy, efficiency, and resolution using a mixed radionuclides standard supplied by International Atomic Energy Agency (IAEA). Energy calibration is essential to qualitative analysis, whereas efficiency calibration is required in quantitative evaluations (Idris, 1999).

Any instrument that is to be used as a spectrometer requires calibration from time to time with sources that emit radiation of known energies. Linearity of response with energy is not being taken for granted, although highly desirable, and calibration with several sources over the entire energy in the range of interest is therefore favourable. For gamma-ray measurements with germanium or sodium iodide detectors, the position of photopeak (full energy peak) is relevant for energy measurements.

3.2.1.1 Energy Calibration

The exact identity of photopeak present in the spectrum produced by the detector system is a necessary requirement for the measurement of gamma-emitters. The energy calibration is the establishing of the number of the channels present in a multi-channel analyzer (MCA) or plus height analyzer in relation to gamma-rays energy. This calibration was made by measuring radioactive Amerasham mixed standard for six hours (Table 3.1). The simple relationship used for energy calibration using two points different in energy and channel number is:

$$E_2 = E_1 + (\Delta E/\Delta C) * (C_2-C_1)$$

Where: E_2 is the unknown energy having channel C_2.

ΔE is the difference in energy.

ΔC is the difference in channel.

3.2.1.2 Resolution Calibration

The resolution of the system is the capability of the detector to separate between two adjoined gamma-lines and it is expressed as the full width of photopeak at the half maximum (FWHM). The resolution of the system was checked periodically and it was 1.8 at 1332 keV ^{60}Co line.

3.2.1.3 Efficiency Calibration

An accurate efficiency calibration of the system is essential to quantification analysis of radionuclides present in a sample. It is the relationship between the number of counts and the disintegration rates, and the efficiency of gamma spectrometer is a measure of how many pulses occur for a given number of gamma-rays. The full energy peak and its calculation can be done using the following equation:

$$\varepsilon = R/(S*P)$$

Where: ε is the efficiency.

R is the count rate in count per second.

S is the source intensity.

P is the probability of emission of particular gamma being measured.

Efficiency calibration curve using Amersham mixed radionuclides standard is shown in Fig. (3.2).

Table 3.1: Gamma energies, branching ratios and the half- live of the radionuclides used for γ- system calibration

Nuclide	γ-ray energy (KeV)	Half-live	Branching ratio %
^{214}Am	60	432.7 y	36.6
^{109}Cd	88	463 d	3.6
^{57}Co	122	271d	85.6
^{139}Ce	166	137.66 d	79.9
^{20}3Hg	279	46.6 d	81.5
^{113}Sn	392	115 d	64.17
^{137}Cs	662	30 y	84.62
^{88}Y	898	106.01 d	94.00
^{60}Co	1173	106.61 d	99.35
^{60}Co	1333	1929 d	99.90
^{88}Y	1836	1929 d	99.98

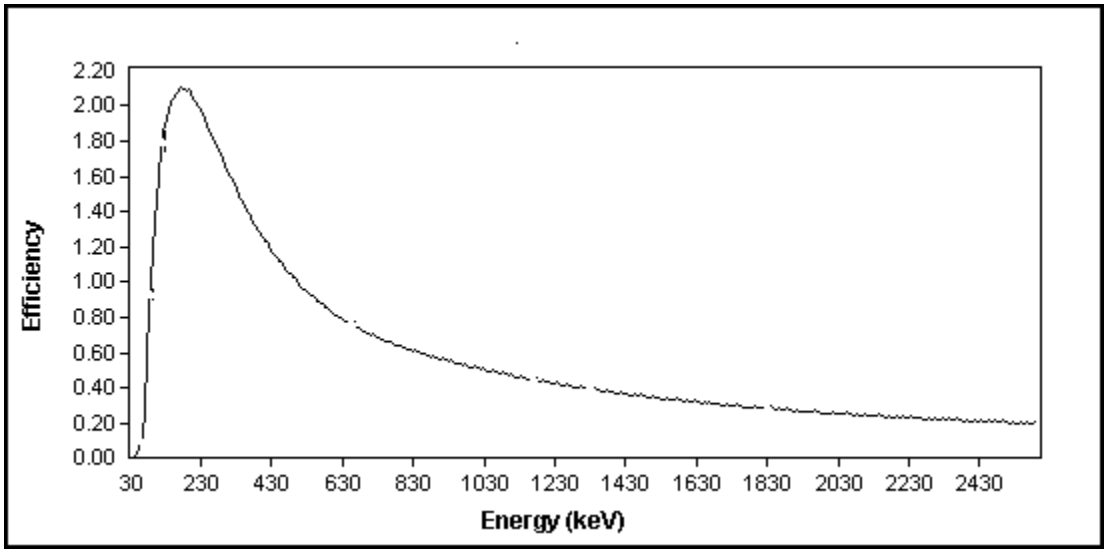

Fig 3.2: Efficiency (%) curve as a function of γ-energy for HPGe detector

3.3 Particle Induced X-ray Emission (PIXE)

Particle induced X-ray emission (PIXE) is by far the most used ion analysis technique in the field of Ion Beam Accelerator (IBA). Johansson *et al*. (1970) presented PIXE as a modern and powerful analytical method. This analytical method soon became widely accepted in different accelerator laboratories, known as PIXE (Particle Induced X-ray Emission) Spectroscopy. Characteristic X-rays produced in sample being irradiated by MeV protons, were for the first time detected by semiconductor Si (Li) X-ray detector that had just become available.

PIXE has four main physical processes of importance, those include: (i) inelastic collisions by sample atoms when a charged particle (proton or heavier ion) enters the material; (ii) decreasing of the energy of the ion along its path according to the specific energy loss (stopping power); (iii) characteristic X-rays are emitted with a probability given by the X-ray production cross section from some of the numerous ionised atoms along the particle path; and finally, (iv) attenuation of X-rays emerging from the sample in the material.

PIXE can be explained as a process composed from two atomic processes :(1) ionization of an inner shell of target atom by the incident ion; and (2) releasing of excess energy by emission of a characteristic X-ray according to the filling of the subsequent electronic vacancy by an outer shell electron.

The production rate of X-rays depends on both the energy of the impinging particle and the atomic number of the target atom. As can be seen in Fig. (3.4), the X-ray yield for Na, Si, Cu and Ba increases with the energy of the beam, but for a fixed beam energy, the X-ray yield decreases steeply with the Z of the target element.

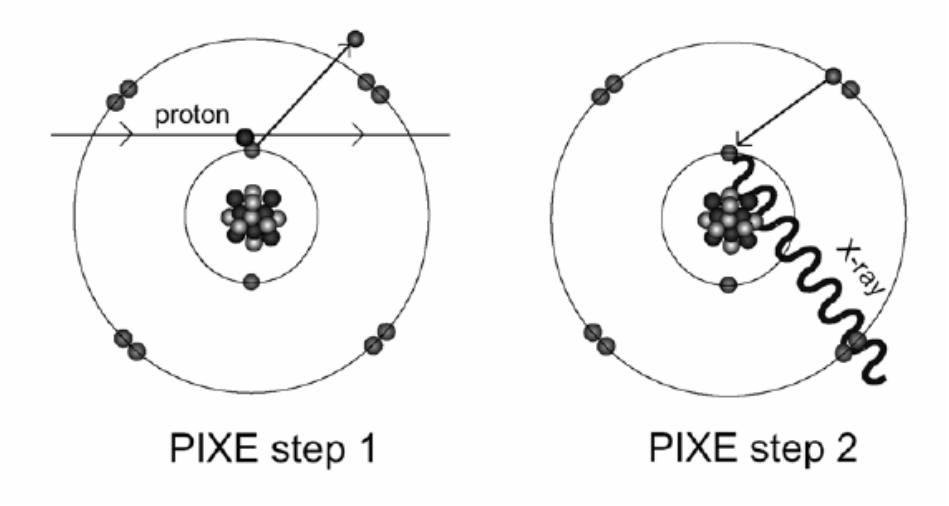

Fig. 3.3: PIXE as a two steps atomic process

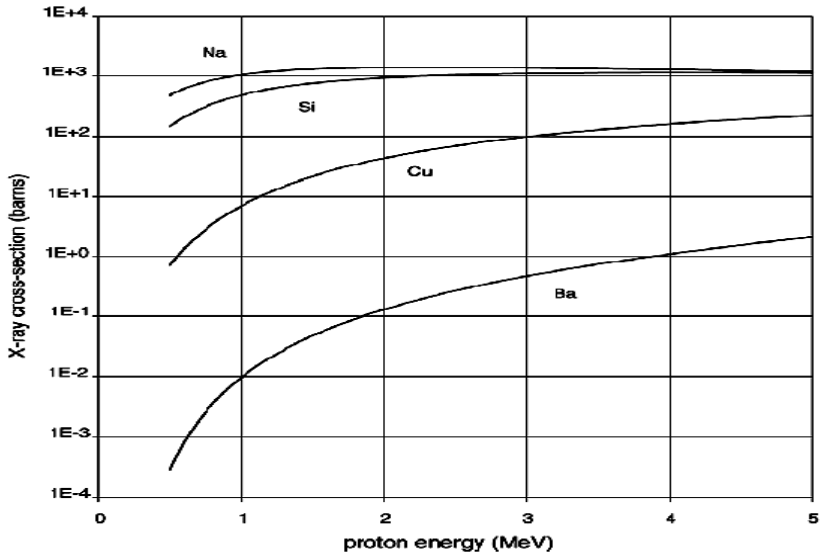

Fig. 3.4: Variations of PIXE yield with energy for various target atoms

For incident proton energy of 1– 4 MeV, elements with atomic number up to about 50 are generally determined through their K x-rays (typically K_α line) Fig. (3.5), whereas heavier elements are measured through their L x-rays Fig. (3.6), because the energies of their K x-rays are too high to be detected by using the Si(Li) detector available commercially, and consequently all elements with Z >11 can be detected simultaneously via either their K or L lines. These characteristics make PIXE suitable for trace element analysis.

By convention, an x-ray line is denoted by a leading capital letter indicating the final shell involved in the transition followed by a small Greek letter and a numeric subscript to reflect the intensity of the line relative to the others (for example $K_{\alpha 1}$). α_1 is the strongest line, α_2 the next and followed by β_1 etc.

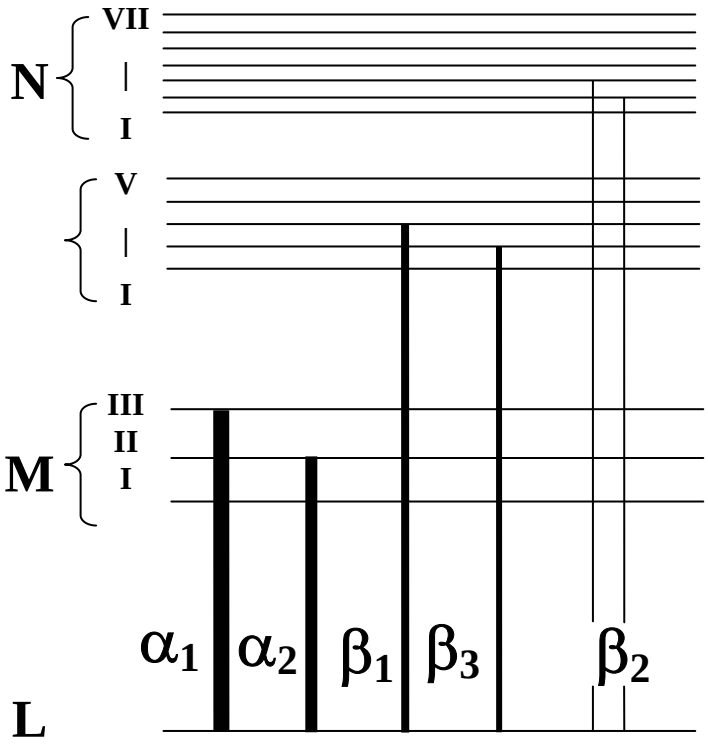

Fig. 3.5: The partial energy level diagram of K X-rays lines

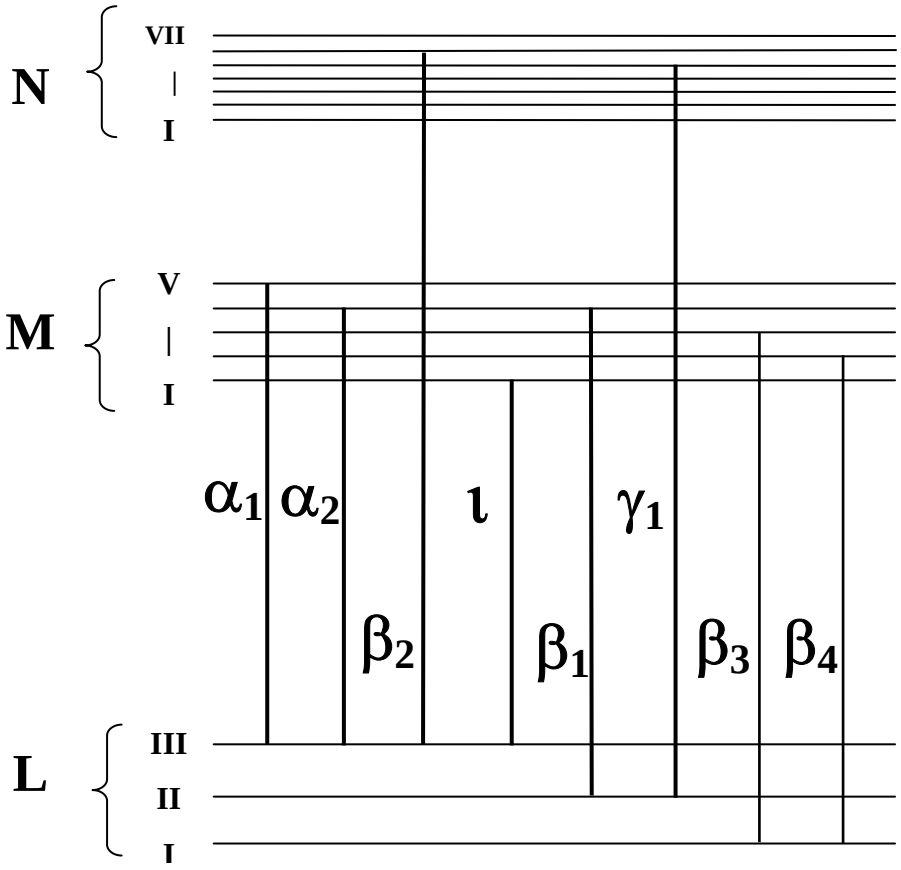

Fig. 3.6: The partial energy level diagram of L X-ray s lines

3.4 Materials and Methods

3.4.1 Hydrology of Study area

The whole of Sudan is drained by the Nile and its two main tributaries, the Blue Nile and the White Nile. The Nile flows for 6.737 kilometers from its farthest headwaters in central Africa to the Mediterranean and the drainage basin of the Nile covers 3,254,555 km²; about 10% of the area of Africa, so considered as the longest river in the world. The importance of the Nile has been recognized since ancient times; for centuries the river has been a lifeline for Sudan.

The Blue Nile flows out of the Ethiopian plateau to meet the White Nile at Khartoum. The Blue Nile is the smaller of the two; its flow usually accounts for only one-sixth of the

total. In August, however, the rains in the Ethiopian highlands swell the Blue Nile until it accounts for 90% of the Nile's total flow. The Blue Nile flows about 1,400 km (850 miles) to Khartoum, where the Blue Nile and White Nile join to form the "Nile proper". 90% of the water and 96% of the transported sediment carried by the Nile originates in Ethiopia, with 59% of the water from the Blue Nile alone. The Blue Nile's two main tributaries, the Dindar and the Rahad, have headwaters in the Ethiopian highlands and discharge water into the Blue Nile only during the summer high-water season. For the remainder of the year, their flow is reduced to pools in their sandy riverbeds (Michael *et al*., 2006).

The White Nile flows north from central Africa, draining Lake Victoria and the highland regions of Uganda, Rwanda, and Burundi. At Bor, the great swamp of the Nile, as Sudd begins. The river has no well-defined channel here; the water flows slowly through this region and much water is lost due to evaporation. The White Nile has several substantial tributaries that drain southern Sudan. In the southwest, the Bahr al Ghazal drains a large basin area. Although the drainage area is extensive, evaporation takes most of the water from the slow moving streams in this region, and the discharge of the Bahr al Ghazal into the White Nile is minimal. In southeast Sudan, the Sobat River drains an area of western Ethiopia and the hills near the Sudan-Uganda border. The Sobat's discharge is considerable; at its confluence with the White Nile just south of Malakal, the Sobat accounts for half the White Nile's water. South of Khartoum, there was the Jabal al Auliya Dam to store the water of the White Nile and then release it in the fall when the flow from the Blue Nile slackens. Much water from the reservoir has been diverted for irrigation projects in central Sudan, however, or it merely evaporates, so the overall flow released downstream is not great.

The United Nile is in Khartoum, the Nile flows through desert in a large (**S**) shaped pattern to empty into Lake Nasser (2,600 miles^2, the world's second largest man-made lake) behind the Aswan High Dam in Egypt. The river flows slowly above Khartoum, dropping little in elevation although five cataracts hinder river transport at times of low water. The Atbara River, flowing out of Ethiopia, is the only tributary north of Khartoum, and its waters reach the Nile for only the six months between July and December. During the rest of the year, the Atbarah's bed is dry, except for a few pools and ponds.

The location of this study select apart of the Nile include (Blue Nile, White Nile and River Nile) in Khartoum state located between 15" 37' N latitudes, and 32" 33' E longitudes with area of about 12416 km^2, because it's the important Sudanese city along the Nile path in the country.

3.4.2 Sample collection and pre-treatment

During the period between November 2005 and June 2006 six field trips were conducted in the White, Blue and River Nile in Khartoum state [*Almourada, Aburoof, Alhittana, Waddelbakheet, Karari, Khor Omer, Alkullia along the River Nile bank; Gar Alnabi, Taibat Alhasanab, Umosher, Waddelagali, Allamab, and Algaba along the White Nile bank; Soba Alhilla, Soba Cabo, Algiraif block 84, Algiraif block 3, Almanshia, Burri, and Garden City along the Blue Nile bank*] and a total of 33 bulk samples from surface River sediments were collected from shallow water in about 15 cm depth. Samples were collected using auger sampler and sometimes with hands and placed in polyethylene bottles with screw caps. In the laboratory samples were sun dried on aluminium trays then gently ground with mortar and pestle to preserve each grain size as it's as possible. The samples of each river were mixed together to get a single homogenized sample and then sieved through 2-mm mesh sieve after which remaining residue was discarded. The homogenized bulk sample was sieved using assembly with pore diameters 2000, 1000, 500, 250, 200, 125 and 100 μm to give sub-samples (fractions). Fractionation was preformed by shaking samples using a mechanical sieve shaker for twenty minutes with the highest velocity of the machine. The homogenized bulk samples from each river (12) and the total of 84 fractions were stored in plastic containers for further analysis.

3.5 Sample Measurements

3.5.1 Gamma-spectrometric measurements

The activity concentration of ^{238}U, ^{232}Th, ^{40}K and ^{137}Cs in the samples were measured using a high resolution γ-spectrometry system equipped with high purity germanium (HPGe) detector with 18% efficiency and u-shape configuration housed in 10 cm lead shield. The detector was calibrated for different geometries using Amersham mixed radionuclide standards (MW 652 for small geometry and MW 651 for large geometry) supplied by International Atomic Energy Agency as displayed in Table (3.1). Suitable

amount of sample, almost 0.5-1 kg, was tightly sealed in a Marinelli beaker with a plastic cover and set a side for four weeks to allow gaseous ^{222}Rn (half-life 3.8 days) and it's short-lived decay products ^{214}Pb (half-life 28.8 minutes) and ^{214}Bi (half-life 19.9 minutes) to reach secular equilibrium with the long lived ^{226}Ra (half-life 1600 years) precursor in the sample.

At the end of the in-growth period the samples were introduced into the lead shielded detector at liquid nitrogen temperature (77 K) and counted for six hours. ^{238}U was analyzed through its progeny peaks: ^{214}Bi (609 keV) and ^{214}Pb (352 keV), while ^{232}Th was analyzed through ^{228}Ac (911 keV) and ^{208}Tl (583 keV) peaks. The activity of ^{40}K and ^{137}Cs was measured directly via 1461 keV and 662 keV peaks, respectively. An empty polyethylene container for each geometry was counted in the same manner as the sample to determine the background distribution around the detector (Sam, 1998). The certified reference material (Whey powder) supplied by International Atomic Energy Agency (IAEA) was used as a quality control sample and the results show good agreement between measured and certified values (relative error calculated was < 10%).

3.5.2 PIXE measurements

For PIXE measurements additional treatment for samples was done to ensure complete dryness of the samples. Samples were placed in an oven overnight at 105º C and pressed into pellets using an electrical compressor and coated with a weightless layer of carbon using carbon coating system for electrical conductivity. The pellets were put in multi-position target holder in a vacuum chamber which can accommodate up to 16 samples. 3 MeV of proton beam with 15 nA current was obtained from 5SDH 1.7 MV Pelletron tandem accelerator. The beam with approximately 5 mm diameter fall onto the target, the average measuring time for the individual sample was 20 minutes. The emitted X-rays were detected using silicon- lithium detector Si(Li) with 30 mm^2 active area and a resolution of 170 eV as Full Width at the Half Maximum (FWHM) at Mn K_α (5.9 KeV), located at 135º with respect to the beam direction in the horizontal plane. A filter of Al (230 μm) with a hole in the center called funny filter (ff) was inserted between the target and Si(Li) detector to suppress the X-ray emitted by elements with Z< 25. The associated electronics include a plus optical preamplifier and amplifier connected to a multi-channel analyzer and computer system. The X-ray spectrum was saved and analyzed using

GUPIX (an interactive software package used to analyze and convert raw spectral data into elemental concentrations) in off-line mode.

Analytical quality control is an essential part for the procedure. The quality control of PIXE was checked by analyzing different soil reference materials (Geostandards BE-N and DR-N) which prepared as the samples and the relative error was within the acceptable limits (Roumie *et al*., 2004; Nsouli *et al*., 2004).

Chapter Four

Result and Discussion

For the ease of reference the results obtained here for radionuclides and heavy metals in different fractions of surface sediments from Blue, White and the River Nile are discussed under subheadings detail of which will be given below.

4.1 Radionuclides

4.1.1 Activity concentration levels

The results of measurements of activity concentration (Bq kg^{-1}) of U-238, Th-232, K-40 and the fallout nuclide Cs-137 in sediments fractions (<100 – 2000 μm) obtained from White Nile, Blue Nile and the River Nile as well as concentration (ppm) of some heavy metals namely, Mg, Ca, Fe, Mn, Ni, Cu, Pb and Zn are presented in Tabular forms and graphs and will thus be discussed below.

Table 4.1 shows the statistical summary for activity concentrations of the above mentioned radionuclides in different grain sizes (<100- 2000 μm) of surface sediments in the three study sites. U-238 activity concentration falls within the range of 5.93- 29.10 Bq kg^{-1} with a mean value of 17.90±5.23 Bq kg^{-1} in the White Nile, 8.84- 29.11 Bq $kg^{-1}$with a mean value of 19.56±5.04 Bq kg^{-1} in the Blue Nile and 14.21- 24.29 Bq kg^{-1} with a mean value of 19.27±2.88 Bq kg^{-1} in the River Nile surface sediments. It is apparent that the mean uranium concentration in different grains sizes is typical in Blue, White and river Nile sediments. This confirms that the River Nile sediments are mixture from Blue and White Nile. It should be in place to note that the minimum value measured in the River Nile sediment almost equal to the sum of minimum values obtained in both Blue and White Nile.

Th-232 activity concentration in different grain sizes ranged from 6.17- 27.22 Bq kg^{-1} (16.38±5.34 Bq kg^{-1}) in the White Nile, 7.00- 26.22 Bq kg^{-1} (17.72±4.69 Bq kg^{-1}) in the Blue Nile and 12.60-22.80 Bq $kg^{-1}$with a mean value of 17.48±2.78 Bq kg^{-1} in the River Nile surface sediments. The argument stated above for uranium applies well for thorium activity concentration, indicating similar geochemical behavior for both elements in the

sediments. It might also be useful to recall that they belong to actinide group of elements with similar radii.

On the average, the ratio between U-238 and Th-232 activity concentration is greater than unity 1.09 in White Nile, 1.13 in Blue Nile and 1.10 in River Nile sediments. This is an indication that there is relative enrichment of uranium over thorium in these sediments.

K-40 activity concentration falls within the range of 6.17- 27.22 Bq kg^{-1} (379.82±107.76 Bq kg^{-1}) in the White Nile, 209.77- 624.15 Bq kg^{-1} (494.36±105.79 Bq kg^{-1}) in the Blue Nile and 292.43- 692.79 Bq kg^{-1} (359.50±83.15 Bq kg^{-1}) in the River Nile surface sediments.

The activity concentration of fallout nuclide Cs-137 in different grain sizes of surface sediments in the study area was measured and found in the range of 0.3- 2.88 Bq kg^{-1} (0.89±0.96 Bq kg^{-1}) in the White Nile, 0.71-6.98 Bq kg^{-1} (3.60±1.55 Bq kg^{-1}) in the Blue Nile and 1.73- 5.6 Bq kg^{-1} (3.02±0.77 Bq kg^{-1}) in the River Nile surface sediments. It must be mentioned that the average Cs-137 activity concentration in the White Nile sediments is one order of magnitude lower than in the Blue and River Nile. Cs-137 levels in the Red Sea coastal sediments ranged from 0.8 to 18.54 Bq $kg^{-1}$with an average of 4.12 Bq kg^{-1} (Sam *et al*., 1998b), and 0.09 ± 0.06 (min) to 4.64 ± 0.19 (max) Bq kg^{-1} in sediments from Karnaphuli river estuary (Alam *et al*., 1997).

Table (4.2) demonstrates the comparison of data obtained in this study with similar data reported from Karnaphuli river estuary in the Bay of Bengal (Alam *et al*., 1997), east and west banks of the River Nile in Upper Egypt (Uosif 2006), and Balochistan Coast in Pakistan (Akram *et al*., 2006a).

Table 4.1: Statistical summary of activity concentration (BqKg^{-1}) for ^{238}U, ^{232}Th, ^{40}K and ^{137}Cs in different grain sizes in sediments from White, Blue and River Nile (No. 96 samples)

Location	Statistical summary	^{238}U	^{232}Th	^{40}K	^{137}Cs
White Nile	Mean ± std	17.91±5.23	16.38±5.34	379.82±107.76	0.88±0.96
	Min	5.93	6.17	154.48	0.30
	Max	29.10	27.22	582.58	2.88
Blue Nile	Mean ± std	19.56±5.05	17.72±4.69	494.37±105.79	3.60±1.55
	Min	8.84	7.00	209.77	0.71
	Max	29.11	26.22	624.15	6.98
River Nile	Mean ± std	19.28±2.88	17.49±2.78	389.51±83.15	3.02±0.77
	Min	14.21	12.60	292.43	1.73
	Max	24.29	22.80	389.51	3.02

Note: full data tables are given in appendix

Table 4.2: Comparison of activity concentration (Bq kg^{-1}) obtained in this study with some data

Location	^{238}U	^{232}Th	^{40}K	Reference
Karnaphuli river (Bengal)	5.87 ± 1.21 to 27.85 ± 1.71	10.44 ± 2.31to 64.02 ± 8.13	118.28 ± 19.70 to 608.21 ± 75.70	Alam et al. 1997
River Nile (Egypt)	52 ± 7.3	76.2 ± 6.2	351.9 ± 17.6	Uosif 2006
Balochistan Coast(Pakistan)	14.4 ± 2.5 to 36.6 ± 3.8	9.8 ±1.2 to 35.2 ± 2.0	144.6 ± 9.4 to 610.5 ±23.9	Akram et al. 2006a
Present study				
i. River Nile	19.27±2.88	17.48±2.78	359.50±83.15	
ii. White Nile	17.90±5.23	16.38±5.34	379.82±107.76	
iii. Blue Nile	19.56±5.04	17.72±4.69	494.36±105.79	

4.1.2 Correlation between activity concentration and grain size

The comparative study of activity concentration of U-238, Th-232 and K-40 as a function of sediment's grain size from the three study sites was performed and presented in Figs 4.1- 4.9. The overall trend there is an increase in activity with decreasing in particle size for uranium, thorium and potassium in both White and Blue Nile. However, the increase in activity with particle size is sharper for uranium relative to thorium. This trend could be explained by the fact that the smaller the particle size the bigger the surface area hence more ion exchange capacity and greater adsorption (Rickert *et al*., 1977; Wilber and Hunter, 1979 and Sam *et al*., 1998a).

Upon comparing location-wise, in Blue Nile the fluctuation in activity concentration for all radionuclides was obvious in contrast to the while Nile, Figs. 4.4-4.6 with noticeable decline in the grain size 200-125 μm and this probably due to depletion in binding substrate which could be an organic matter or ferric-manganese oxides in this fraction since they are the two main components of sediments responsible for adsorption of radionuclides and play the role of sorption substrate in surface sediments (Sam, 1998). On the other hand, in the River Nile sediments as presented in Figs. 4.7-4.9. there seems no clear trend between activity concentration and the grain size as seen in the sediments of its tributaries. We don't have clear explanation as why the River Nile sediments display such exceptional behavior which is contrary to that met with sediments of White and Blue Nile.

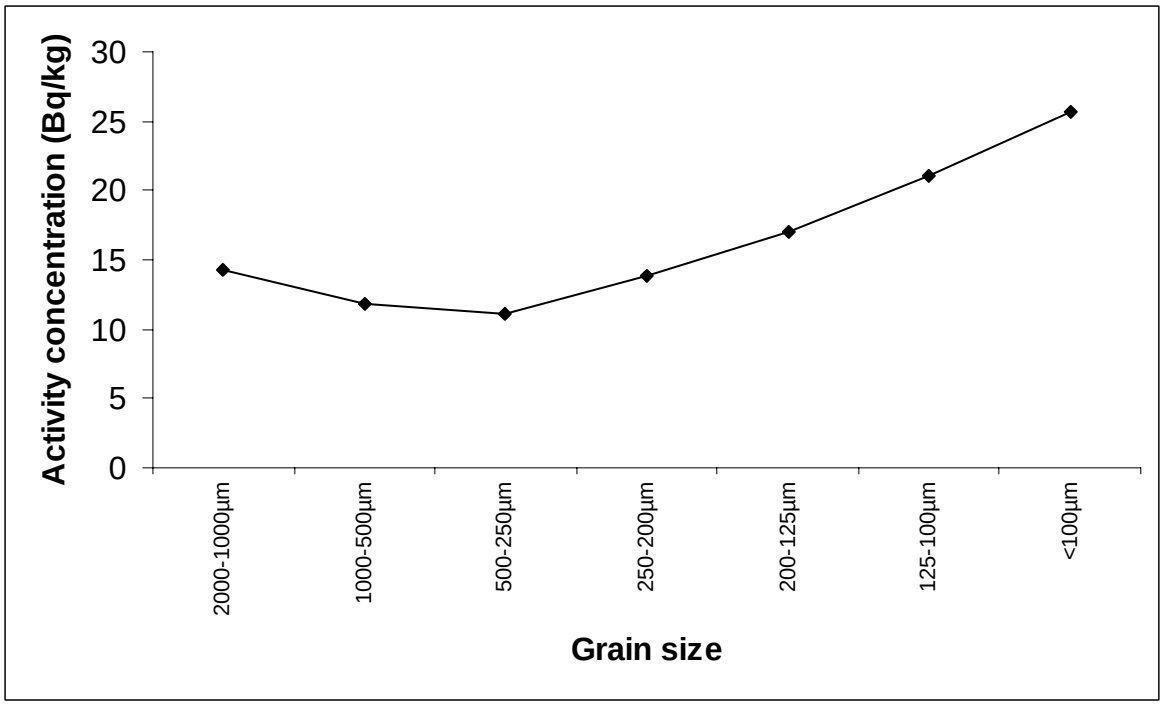

Fig. 4.1: Relationship between ^{232}Th average activity concentration (Bq kg^{-1}) and grain size in White Nile sediments

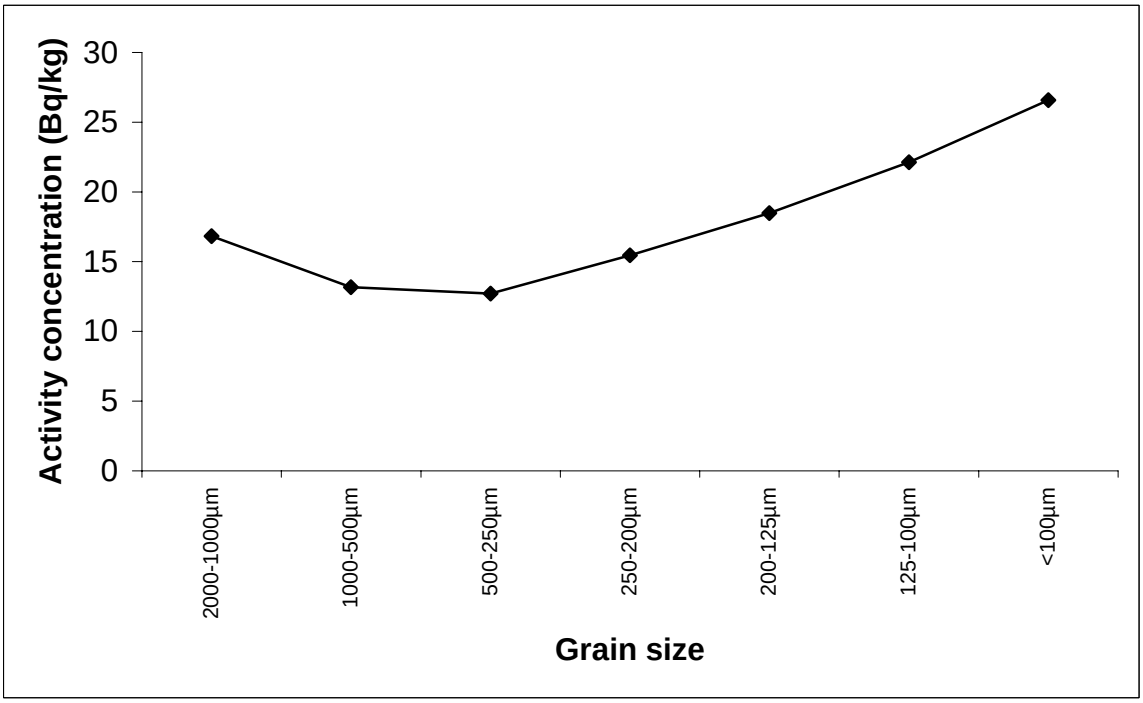

Fig. 4.2. Relationship between ^{238}U average activity concentration (Bq kg^{-1}) and grain size in White Nile sediments

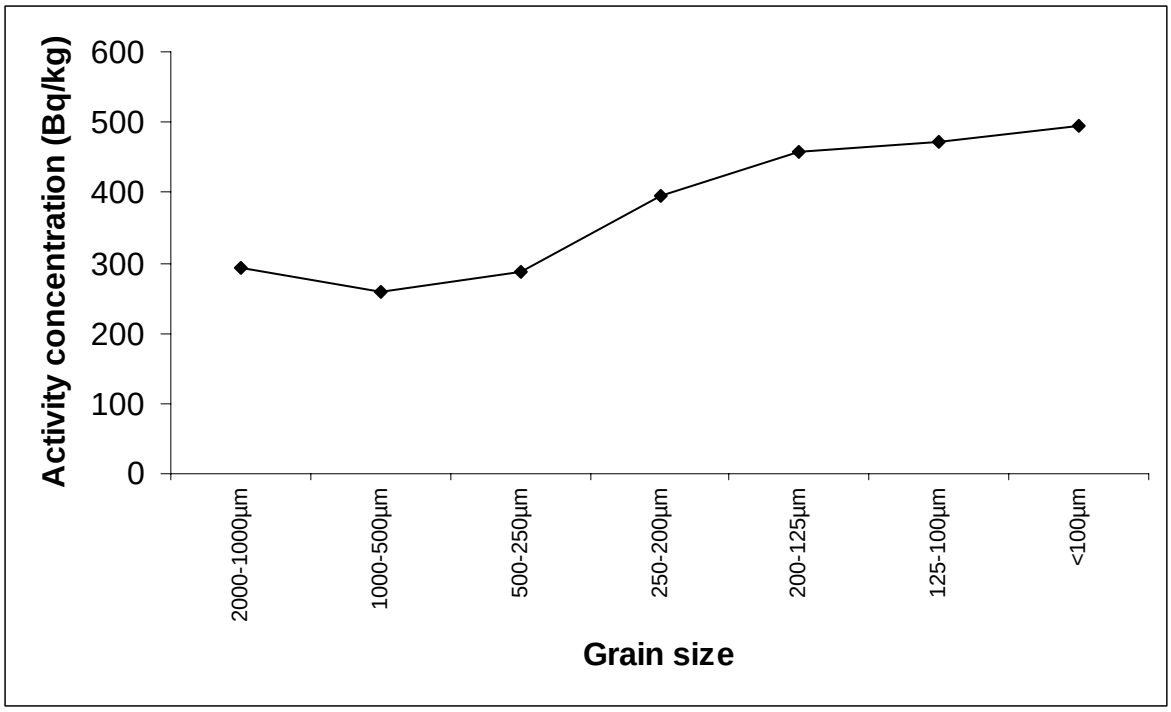

Fig. 4.3: Relationship between ^{40}K average activity concentration (Bq kg^{-1}) and grain size in White Nile sediments

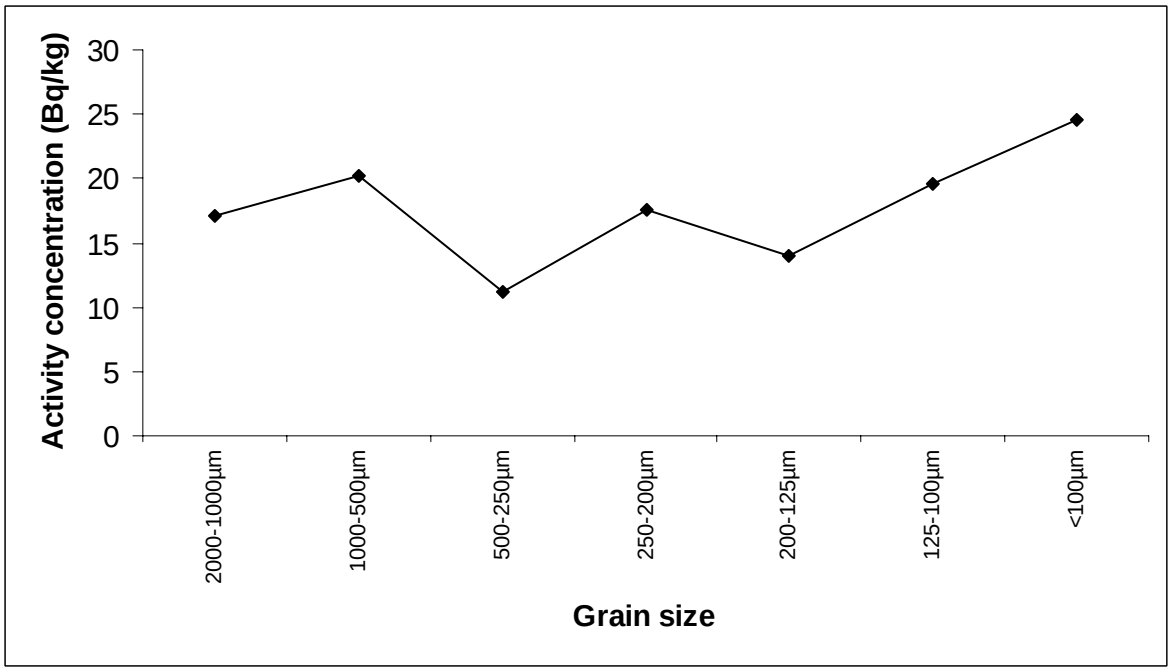

Fig. 4.4. Relationship between ^{232}Th average activity concentration (Bq kg^{-1}) and grain size in Blue Nile sediments

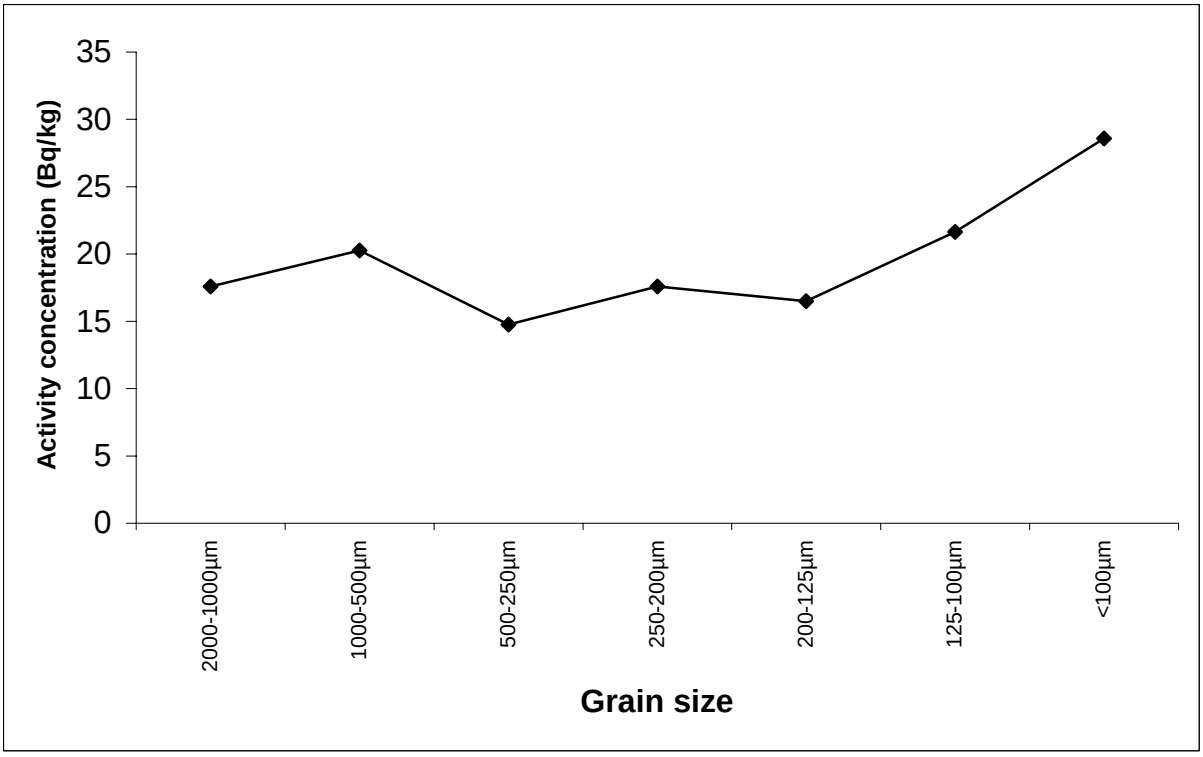

Fig. 4.5: Relationship between ^{238}U average activity concentration (Bq kg^{-1}) and grain size in Blue Nile sediments

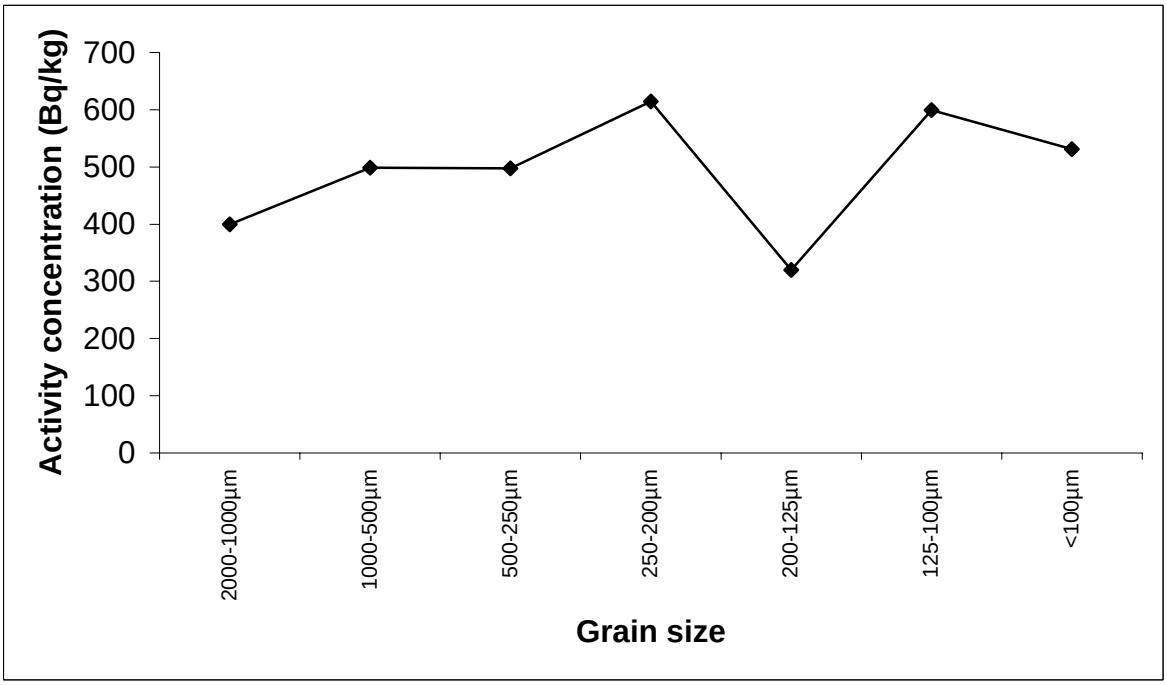

Fig. 4.6: Relationship between ^{40}K average activity concentration (Bq kg^{-1}) and grain size in Blue Nile sediments

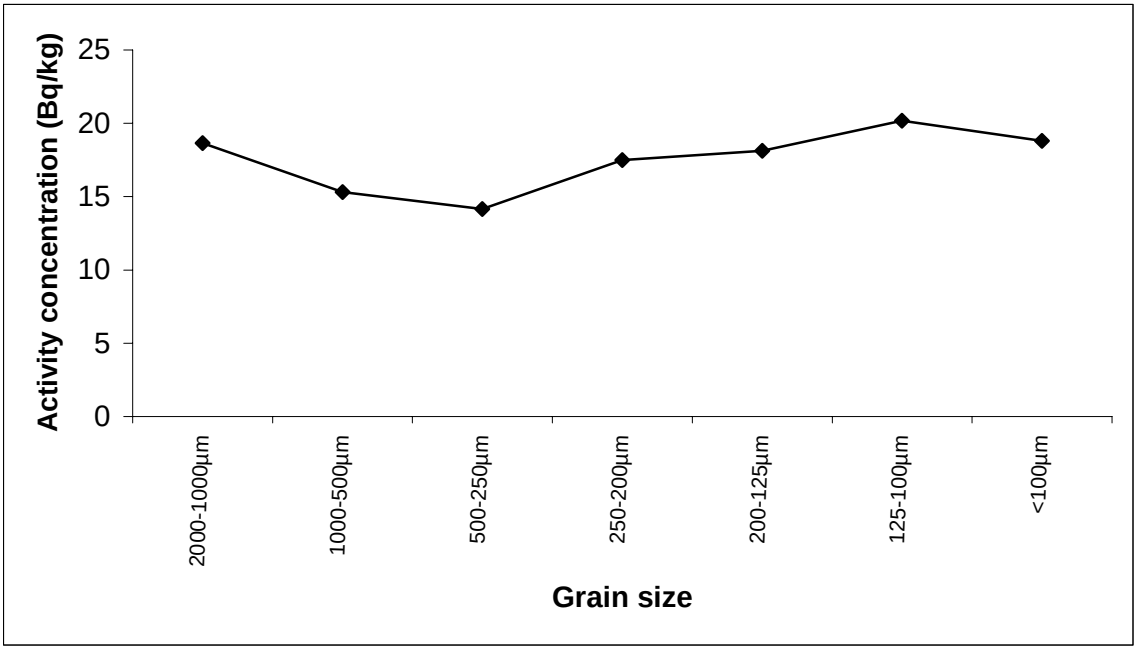

Fig. 4.7. Relationship between ^{232}Th average activity concentration (Bq kg^{-1}) and grain size in River Nile sediments

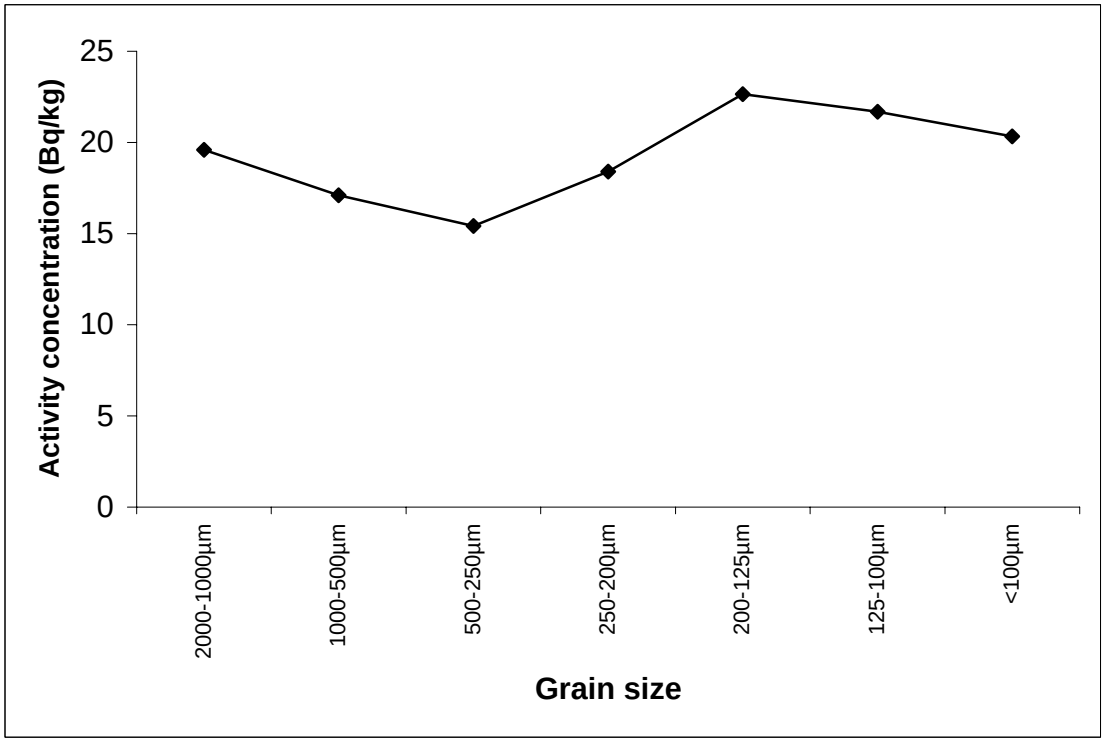

Fig. 4.8: Relationship between ^{238}U average activity concentration (Bq kg^{-1}) and grain size in River Nile sediments

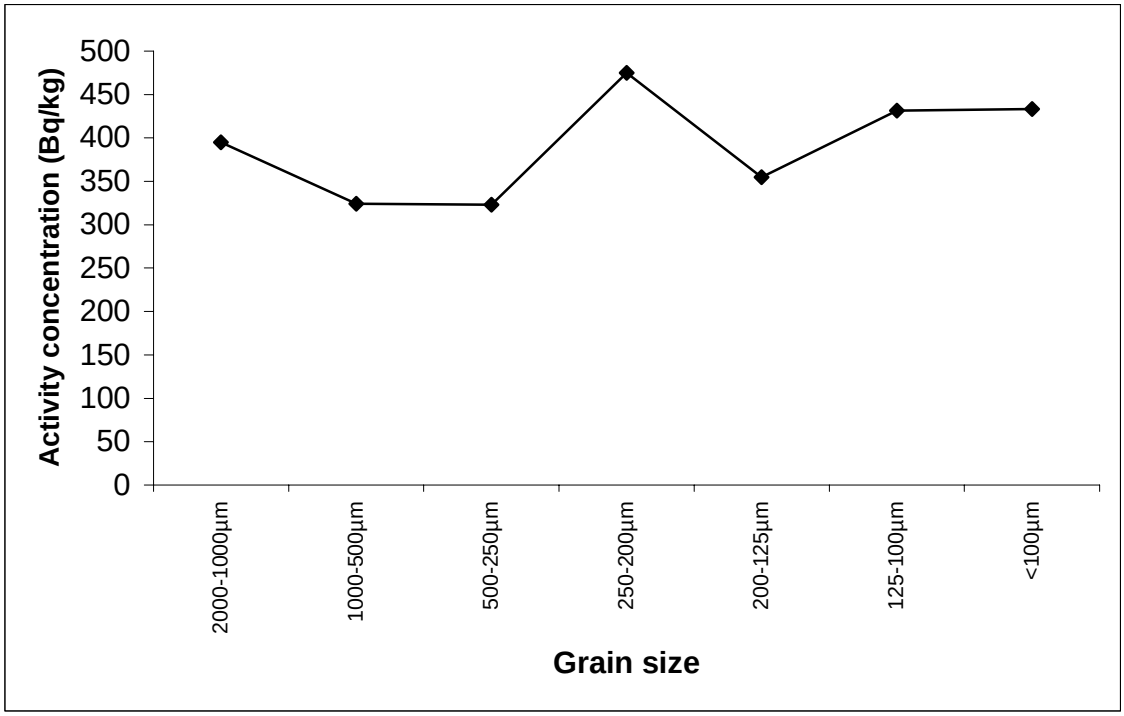

Fig. 4.9: Relationship between ^{40}K average activity concentration (Bq kg^{-1}) and grain size in River Nile sediments

4.1.3 Variation in individual values within single grain size

The study of variation in measured values of activity concentration in the same fraction for each radionuclide in each river was conducted using Whisker's Box Plot and the results are depicted in Figs. 4.10.-4.18.

As can be seen in**,** the activity concentration of U-238 and Th-232 in White Nile sediments behave similarly with small variations in the fine grain sizes (<500) and remarkable scattered in coarse fractions (>500μm). Whereas in the Blue Nile the values are highly varied in grain size 200-125μm for both radionuclides, however, the variation in U-238 activity concentrations tend to be wider than for Th-232. On the contrary, in River Nile sediments Th-232 activity concentration is more scattered than for U-238 in most grain sizes.

From the above it can be observed that, there is a general trend in the White Nile sediments to reflect its behavior as it has a relatively constant flow and quiet move along its stream, this mean there is enough time for sedimentation process to take place throughout the flow and the sediments compose from almost same particles and hence could be classified as homogenous sediments. In the Blue Nile sediments composition is more heterogeneous; this might be related to the behavior of this river as it's affected by the tremendous runoff resulting during rain seasons (June to October) in the Ethiopian plateau, so the content of the sediments in the different fractions may contain different species of silt and clay materials. In River Nile sediments the variation is more pronounce for Th-232 in most grain sizes except in the finest fraction (< 100 μm).

The variation in K-40 activity concentration in Blue Nile sediment fractions is generally small for all fractions except in 200-125 μm, whereas in the White Nile sediments it is wider in most fractions. The trend in the River Nile sediments shows that the variation is remarkable in fraction 200-250 μm.

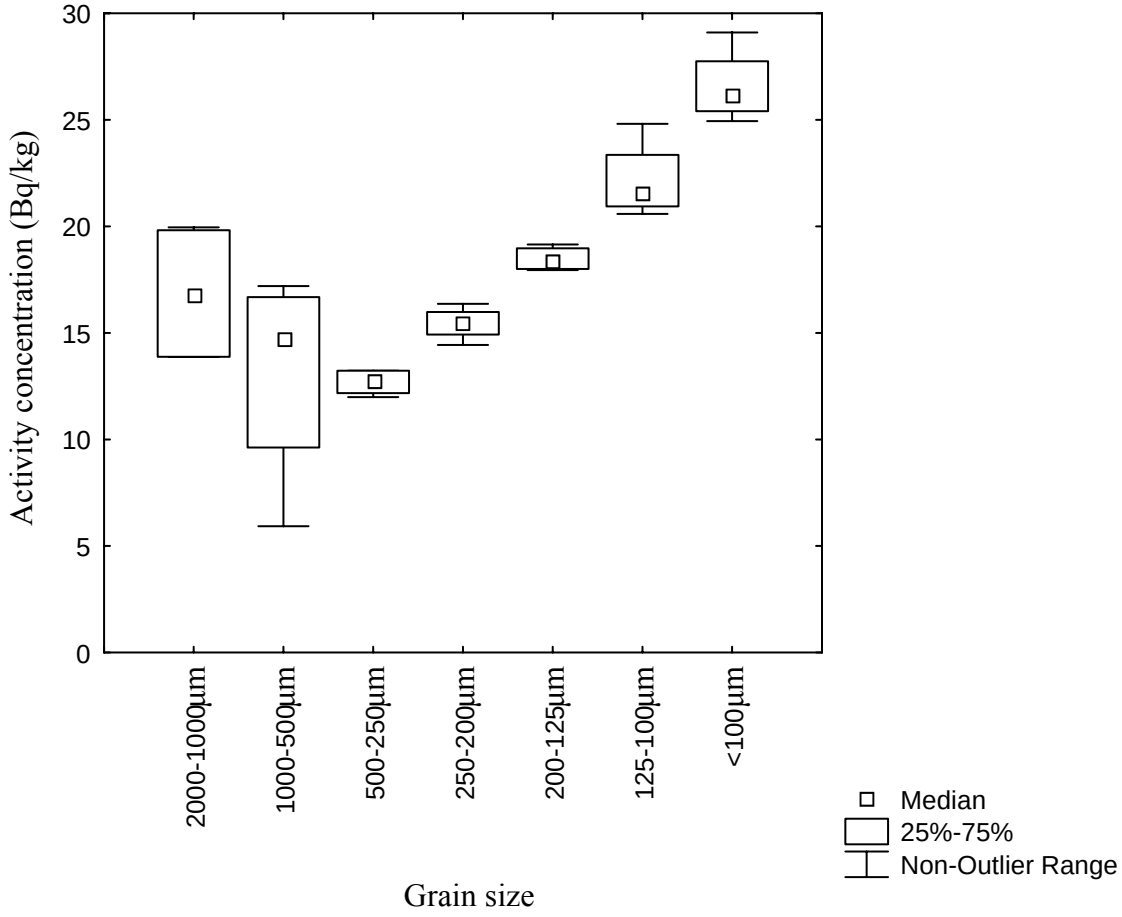

Fig. 4.10: Plot of ^{238}U Activity concentration (Bq kg^{-1}) as a function of single grain size in White Nile sediments

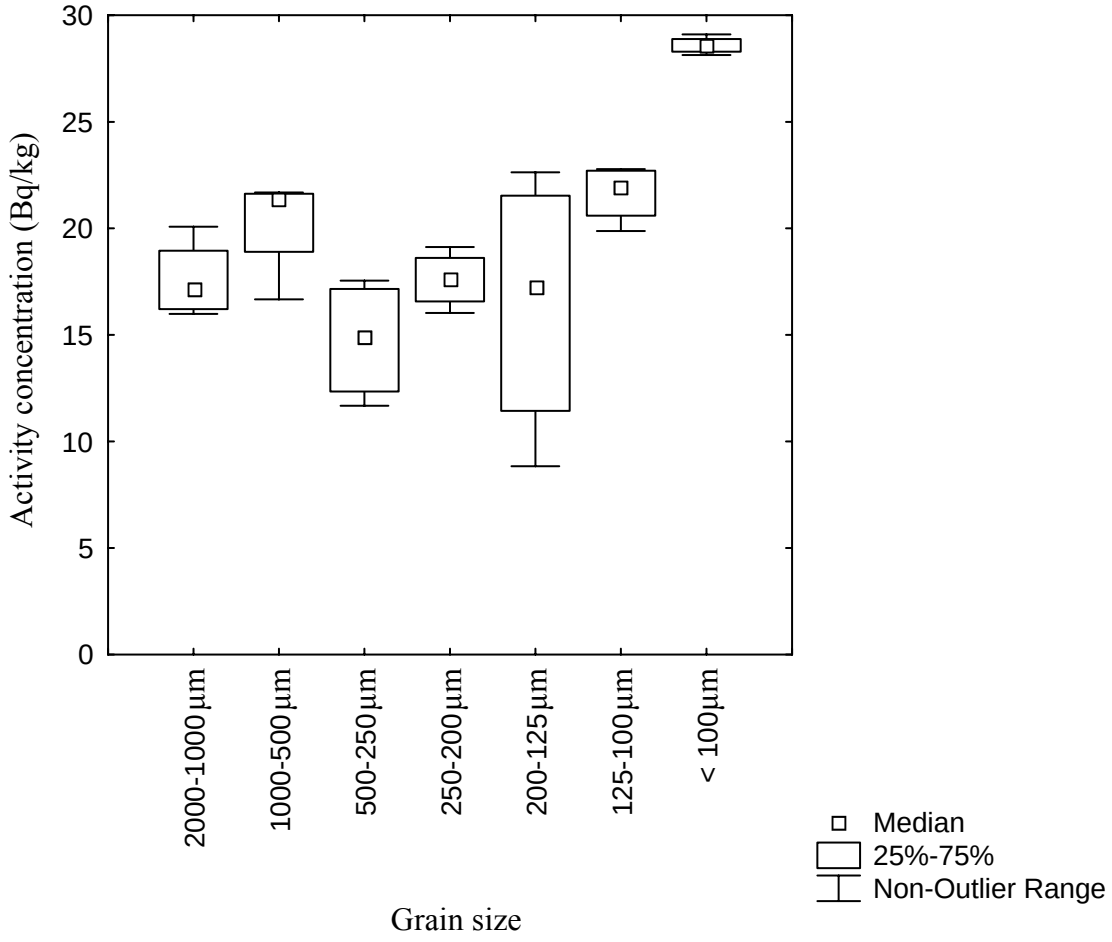

Fig. 4.11: Plot of ^{238}U activity concentration (Bq kg^{-1}) as a function of single grain size in Blue Nile sediments

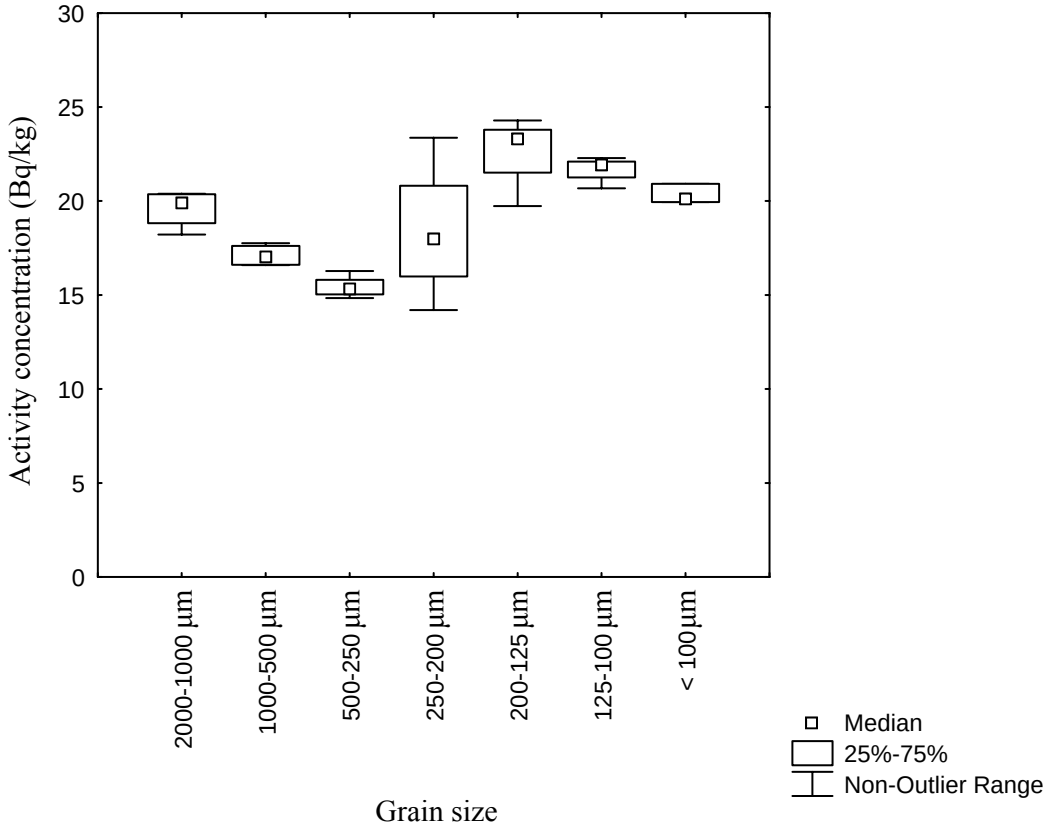

Fig. 4.12: Plot of ^{238}U activity concentration (Bq kg^{-1}) as a function of single grain size in River Nile sediments

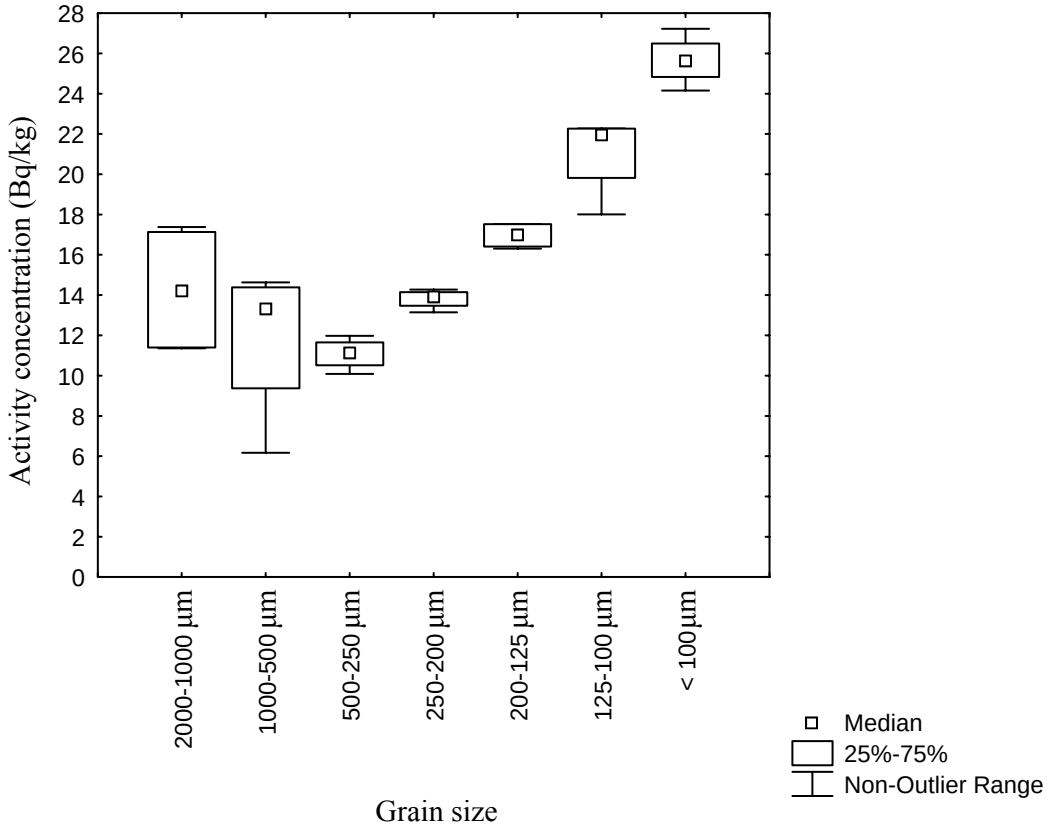

Fig. 4.13: Plot of ^{232}Th activity concentration (Bq kg^{-1}) as a function of single grain size in White Nile sediments

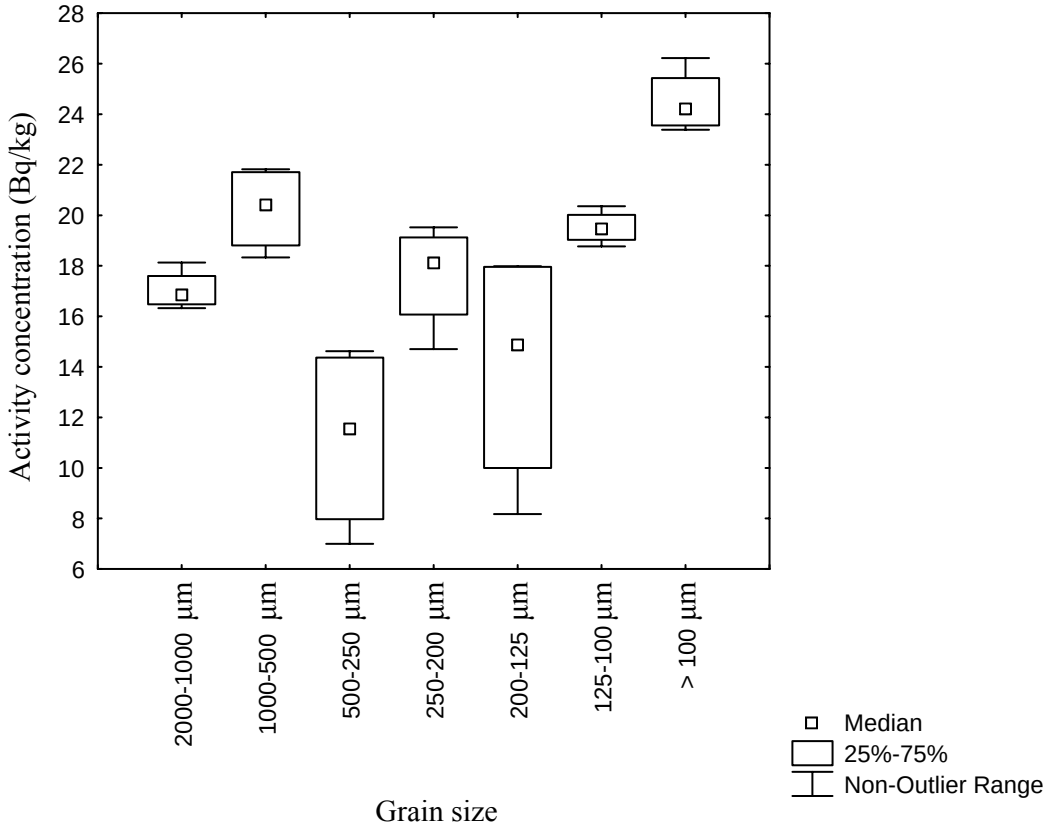

Fig. 4.14: Plot of ^{232}Th activity concentration (Bq kg^{-1}) as a function of single grain size in Blue Nile sediments

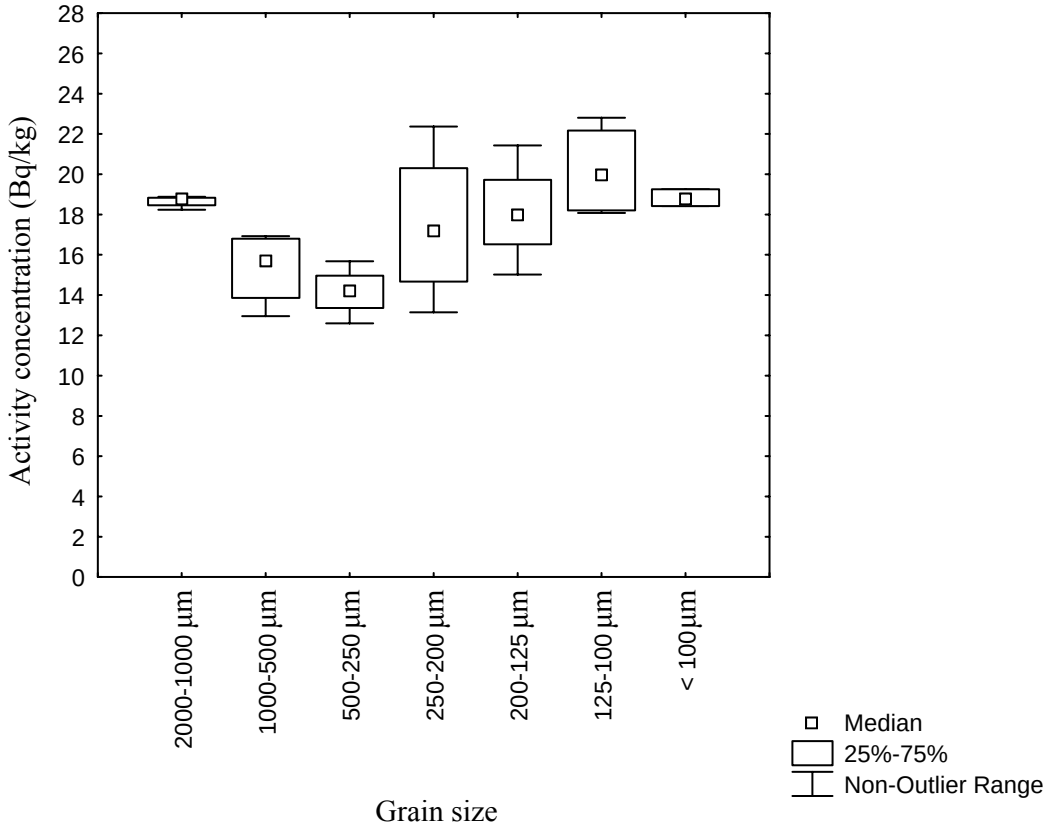

Fig. 4.15: Plot of ^{232}Th activity concentration (Bq kg^{-1}) as a function of single grain size in River Nile sediments

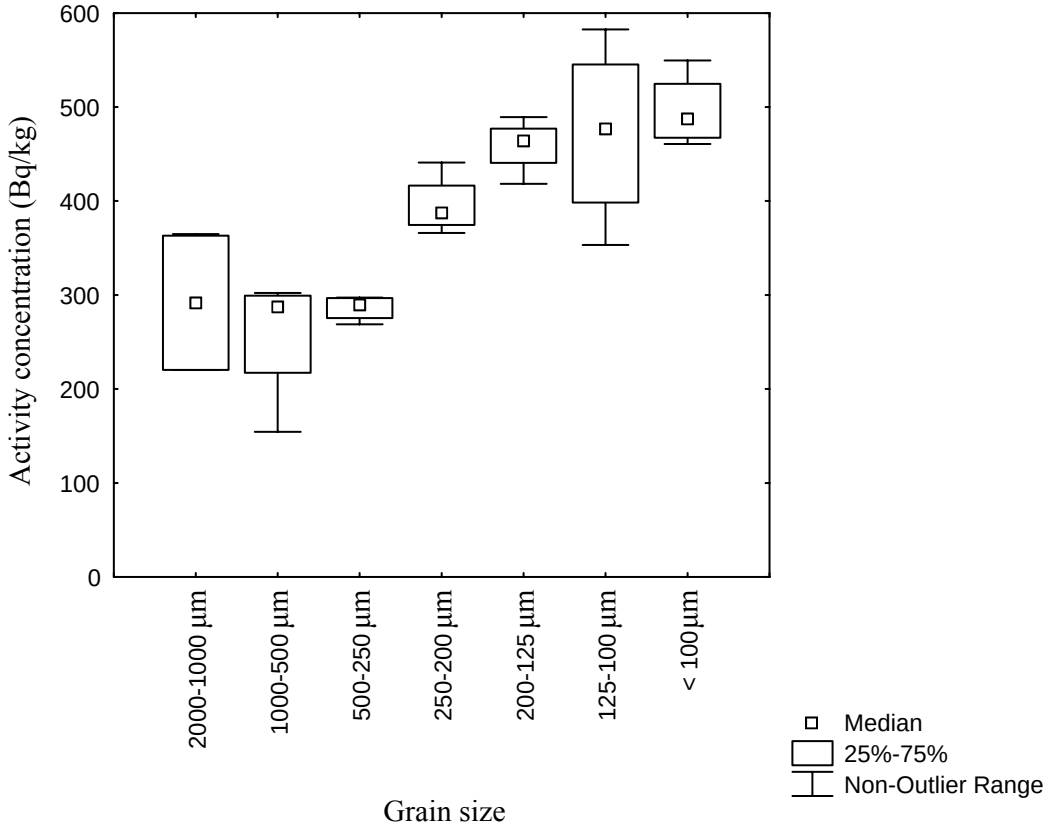

Fig.4.16: Plot of ^{40}K activity concentration (Bq kg^{-1}) as a function of single grain size in White Nile sediments

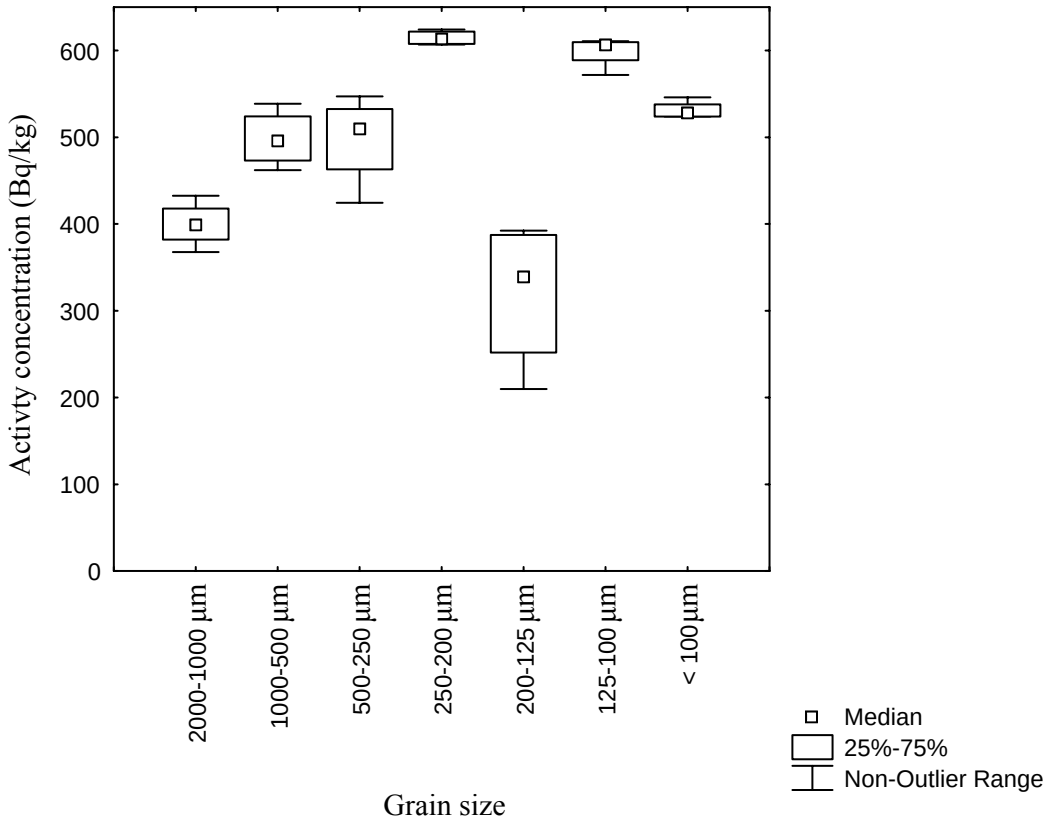

Fig. 4.17: Plot of ^{40}K activity concentration (Bq kg^{-1}) within single grain size in Blue Nile sediments

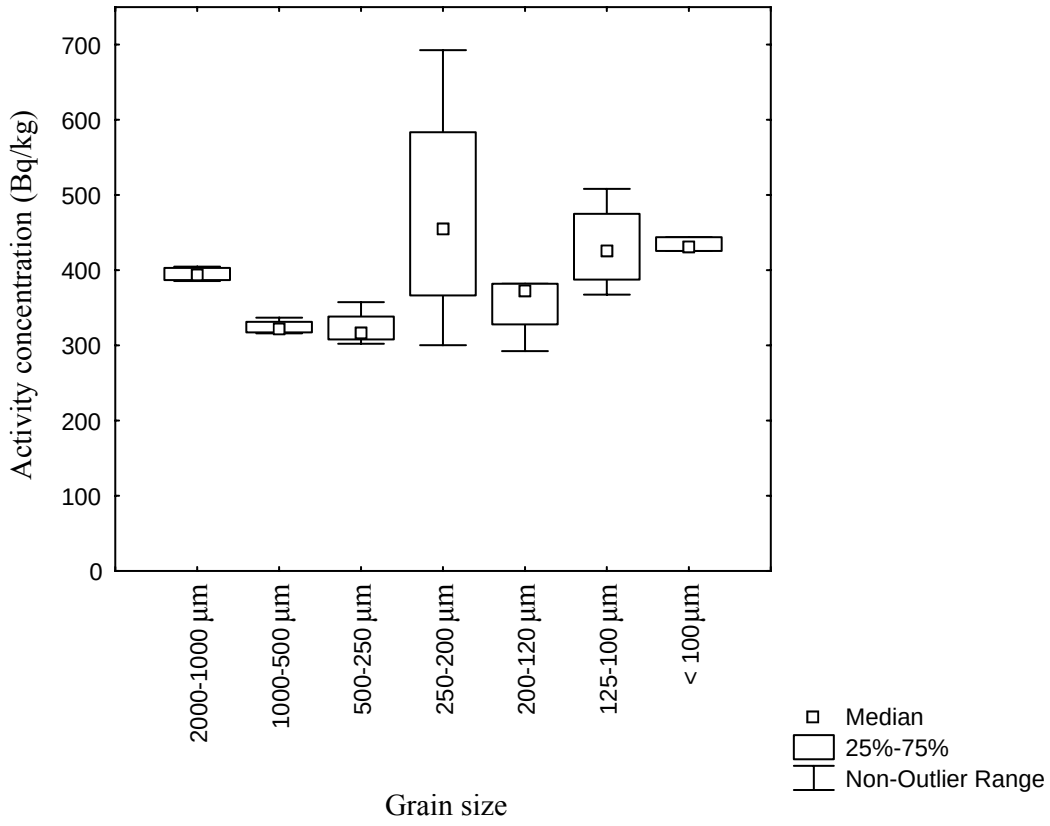

Fig. 4.18: Plot of ^{40}K activity concentration (Bq kg^{-1}) within single grain size in River Nile sediments

4.1.4 The correlation coefficient

Normality test of the data showed that the distribution of the data is normal in all locations of the study area. Based on this further statistical correlation analysis was performed. Fig. 4.19-4.21 illustrate the correlation between the activity concentration of radionuclides and grain size in sediments from White, Blue and River Nile, the correlation is insignificant (R^2 = 0.077 for U-238, 0.052 for Th-232 and 0.133 for K-40). The correlation coefficient as inferred from the nonparametric tests, because the grain size as variable showed non-normal distribution and the values were -0.542 for U-238, -0.462 for Th-232 and -0.371 for K-40, it appears that there is inverse relationship between activity concentration of radionuclides and grain size which further confirms R^2 values.

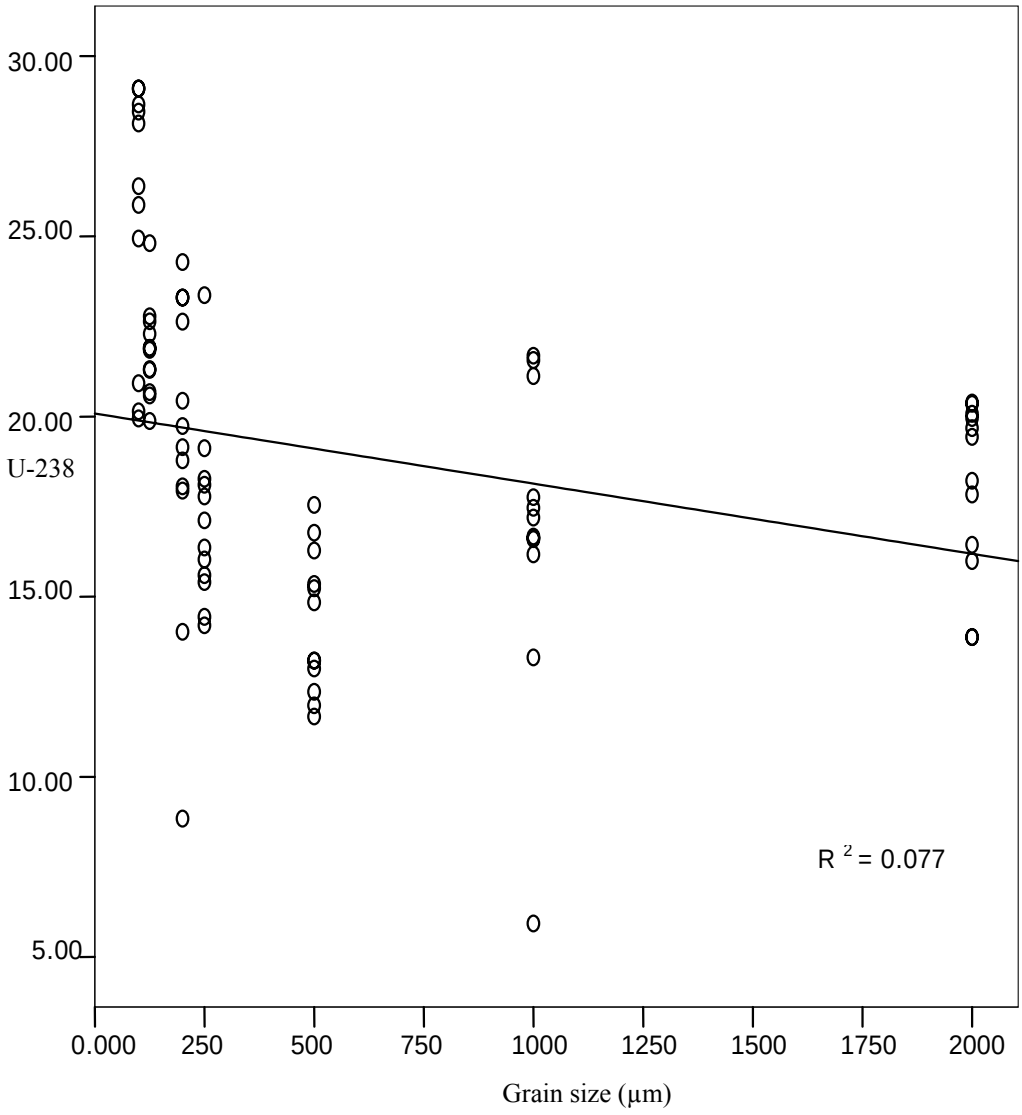

Fig. 4.19: ^{238}U scatter diagram illustrating regression line between grain size and the activity concentration (Bq/kg)

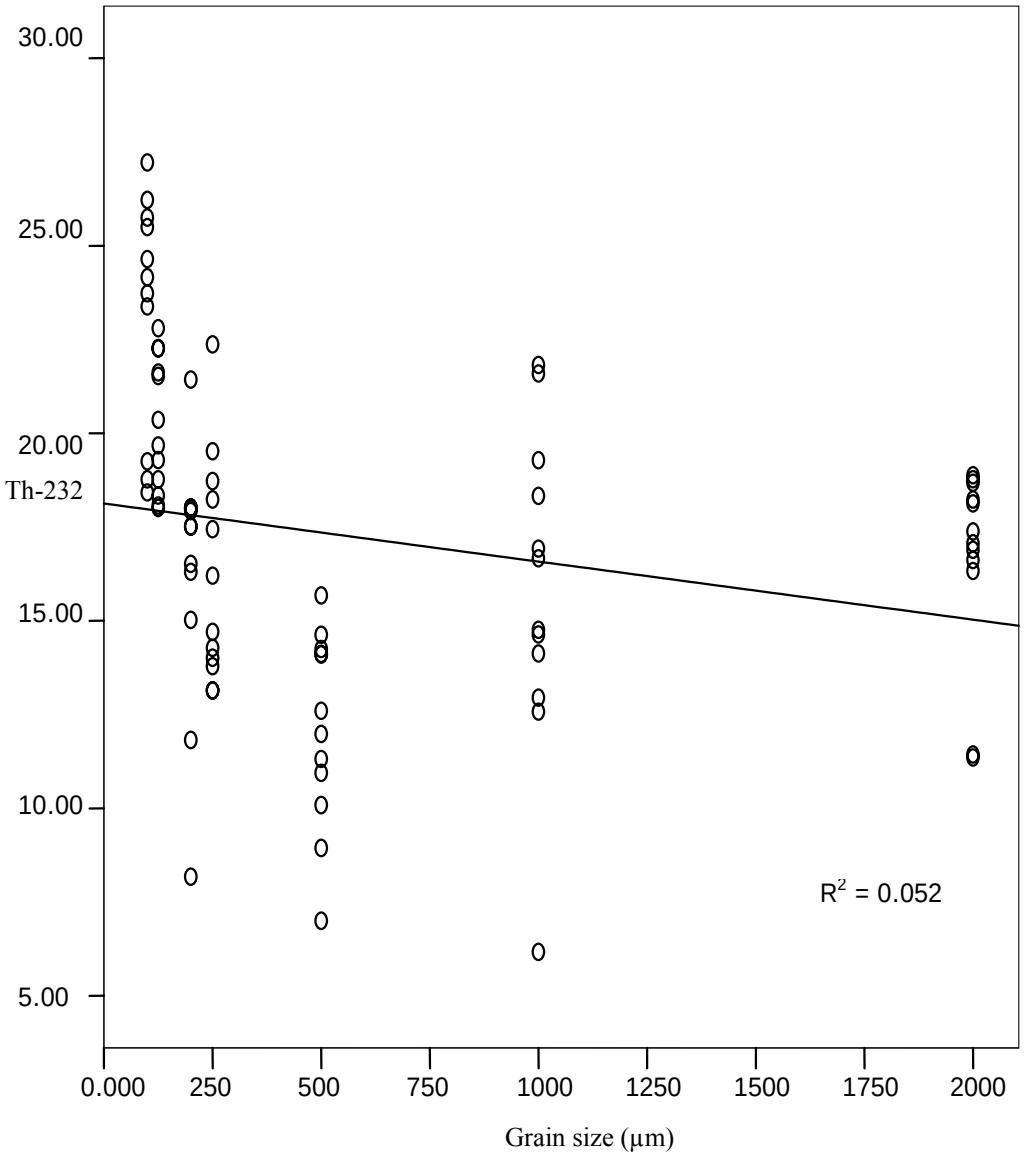

Fig. 4.20: ^{232}Th scatter diagram illustrating regression line between grain size and activity concentration (Bq/kg)

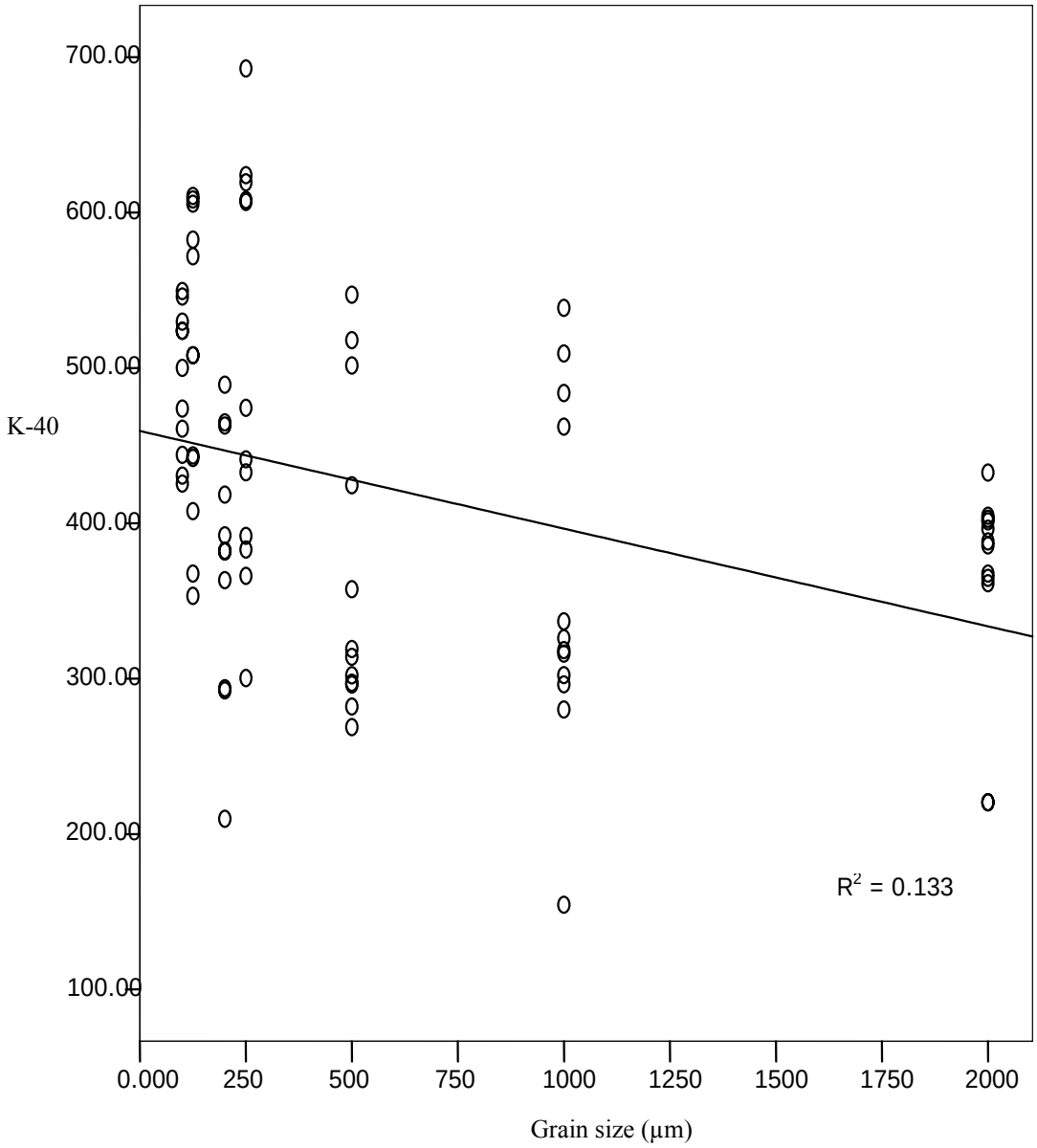

Fig. 4.21: ^{40}K scatter diagram illustrating regression line between grain size and activity concentration (Bq/kg)

4.2 Heavy metals

Statistical summary of concentration (ppm or mg/g dry weight) of magnesium, calcium, manganese, nickel, iron, copper, zinc and lead in different grain sizes (2000µm- <100µm) of surface sediments collected from White, Blue and River Nile within Khartoum state boundaries are shown in Table (4.3).

Table 4.3: Statistical summary of Concentration (mg/g dry weight) for Fe, Ca, Mg and Mn in different grain sizes of sediments from White, Blue and River Nile (No. 48 samples)

Element	Mean ± std	Min	Max	Location
Fe	54.94±8.67	37.80	67.31	White Nile
Ca	34.80±10.67	22.89	51.82	
Mg	14.20±2.13	11.32	18.49	
Mn	1.19±0.33	0.82	1.78	
Fe	90.49±18.78	39.99	106.34	Blue Nile
Ca	35.82±4.35	24.36	41.11	
Mg	12.24±1.90	7.46	14.40	
Mn	1.62±0.25	0.92	1.91	
Fe	87.92±7.13	77.32	98.00	River Nile
Ca	33.70±4.33	28.16	42.02	
Mg	12.00±0.63	10.68	12.79	
Mn	1.61±0.18	1.28	1.87	

Note: full data tables are given in appendix

Table 4.4: Statistical summary of Concentration (µg/g dry weight) for Ni, Cu, Zn and Pb in different grain sizes of sediments from White, Blue and River Nile (No. 48 samples)

Element	Mean ± std	Min	Max	Location
Ni	35.26±14.99	12.77	65.90	White Nile
Cu	32.86±11.16	16.30	54.81	
Zn	74.75±9.82	56.70	91.98	
Pb	8.85±6.12	3.09	32.08	
Ni	49.28±20.78	14.13	84.07	Blue Nile
Cu	61.39±19.58	22.73	90.78	
Zn	116.95±27.01	49.66	150.60	
Pb	12.05±6.02	0.94	19.67	
Ni	48.78±16.49	23.95	76.19	River Nile
Cu	59.72±9.75	38.71	74.59	
Zn	113.33±12.69	94.87	136.90	
Pb	12.80±6.84	1.28	22.06	

Note: full data tables are given in appendix

Based on concentrations encountered in different grain sizes, the elements considered could be classified into two broad categories. Fe, Ca, Mn and Mg are relatively present in high concentrations as depicted in Table (4.3) with the exception Fe in White sediments which display relatively low concentration; on the average the values obtained are similar in all sites. This similarity in concentration of heavy metals in different grain sizes, reflect the crust origin of the sediments and absence of anthropogenic contribution in the sediments (Idris, 1999).

Upon plotting the concentration of each element against grain size in the three rivers as illustrated in Figs.4.22-4.25, it seems that there is no clear relationship between elemental concentration and the particle size. The only noticeable observation is that there is sharp decrease in concentration of the four elements (Fe, Ca, Mn and Mg) in fraction size 500-250 μm.

The other category represents elements (Ni, Cu, Zn and Pb) that reflect low concentrations compared to the elements mentioned above. Table (4.4) show concentration obtained in different grain sizes of sediment of the three rivers. Upon comparing the results location-wise, the results are more or less similar with the exception of Zn which remarkable fluctuation from one site to another. Likewise, there seems no correlation between elemental concentration and grain size (Figs.4.26-4.29).

The comparison between these values of heavy metals concentration with reported data from Mooi River in South Africa (Van and Erdmann, 2004) [Pb 34-62, Zn 25-59 and Cu 11-36 μg/g], shows that the range of lead in the three sites is lower than those found in Mooi River, whereas zinc and copper are higher.

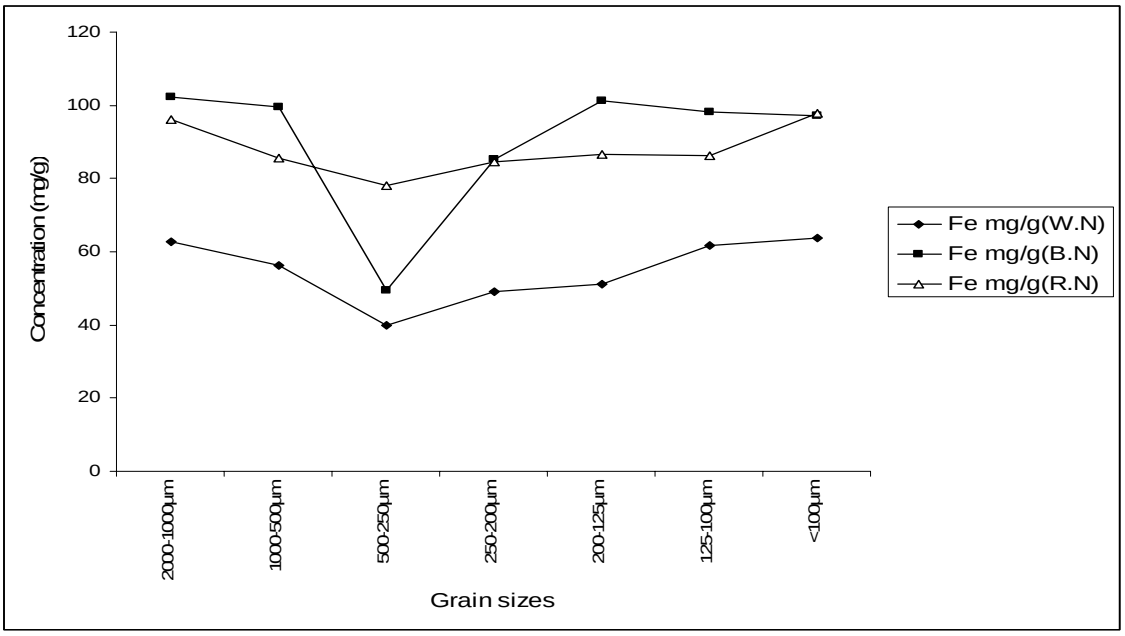

Fig. 4.22: Plot of Fe concentration as a function of sediment grain size in White, Blue and River Nile

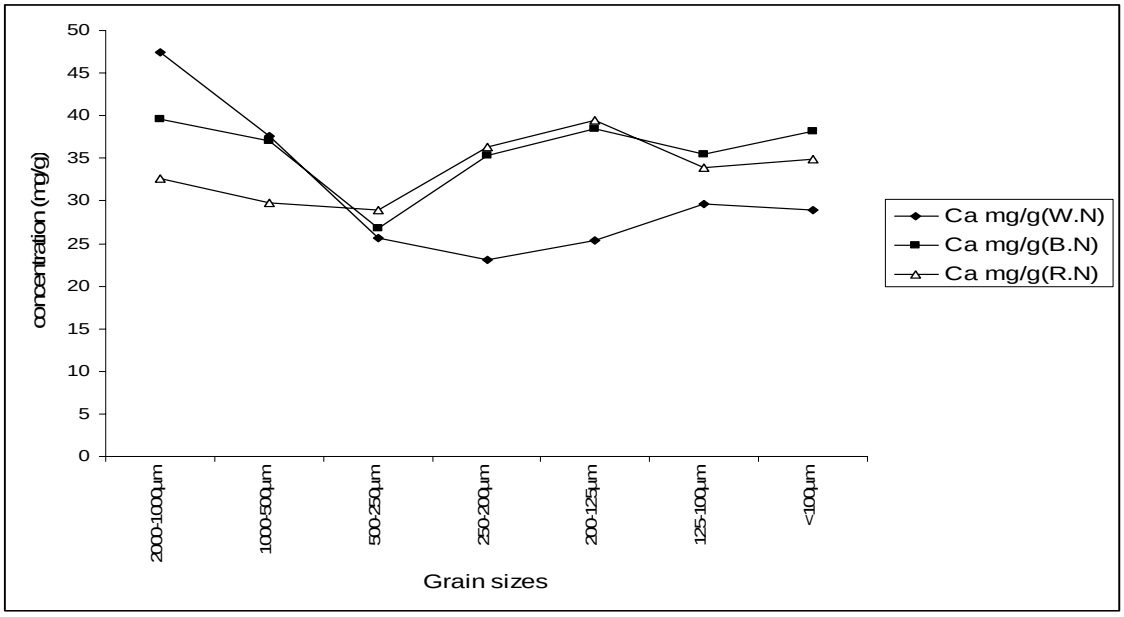

Fig. 4.23: Plot of Ca concentration as a function of sediment grain size in White, Blue and River Nile

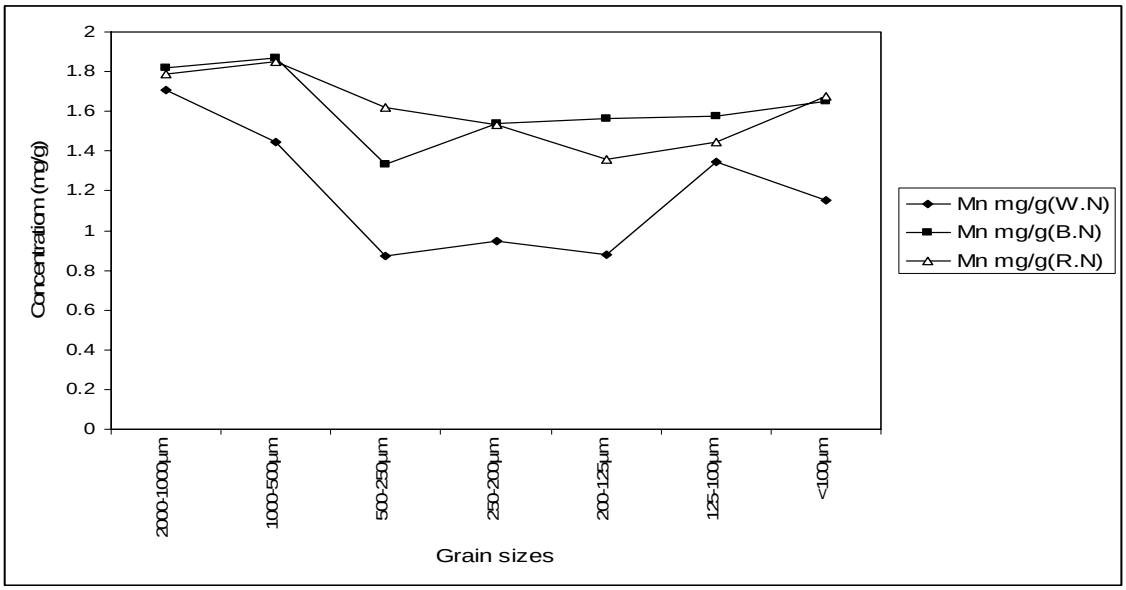

Fig. 4.24: Plot of Mn concentration as a function of sediment grain size in White, Blue and River Nile

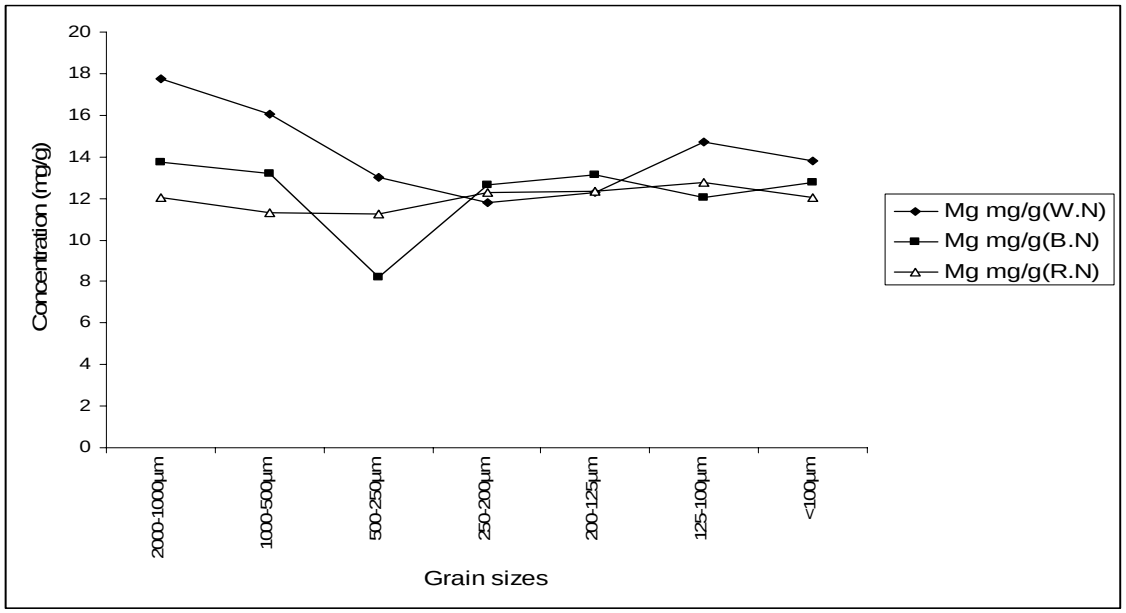

Fig. 4.25: Plot of Mg concentration as a function of sediment grain size in White, Blue and River Nile

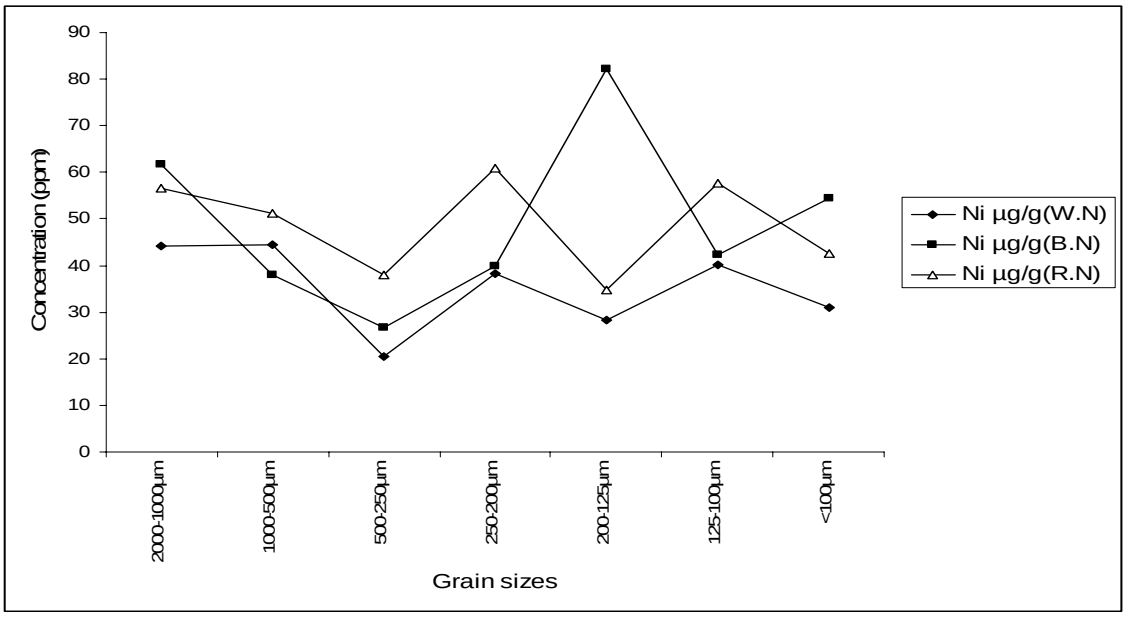

Fig. 4.26: Plot of Ni concentration as a function of sediment grain size in White, Blue and River Nile

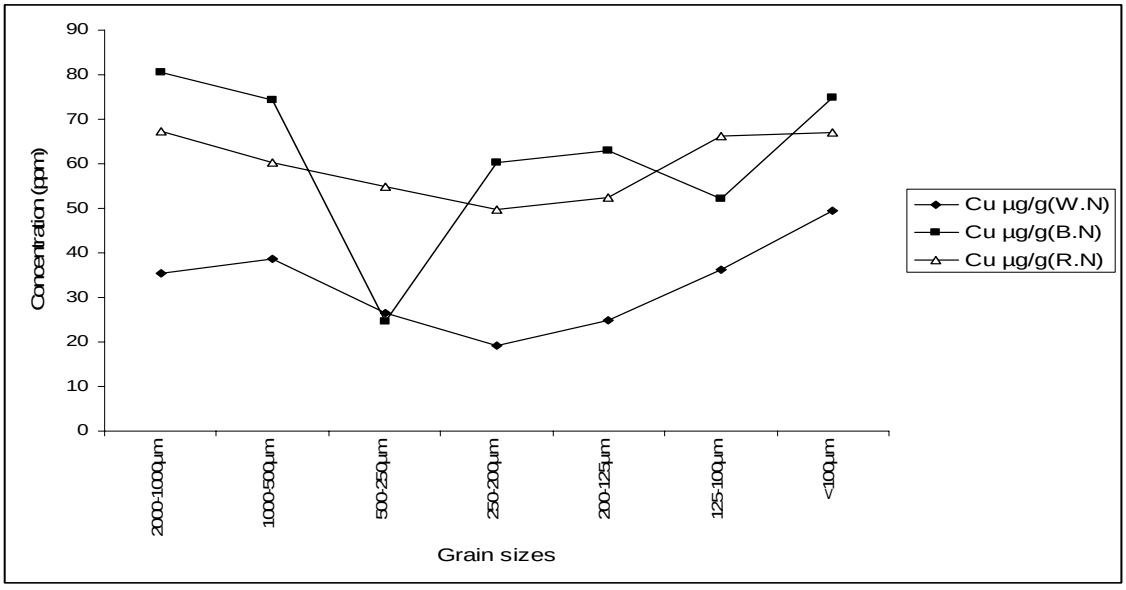

Fig. 4.27: Plot of Cu concentration as a function of sediment grain size in White, Blue and River Nile

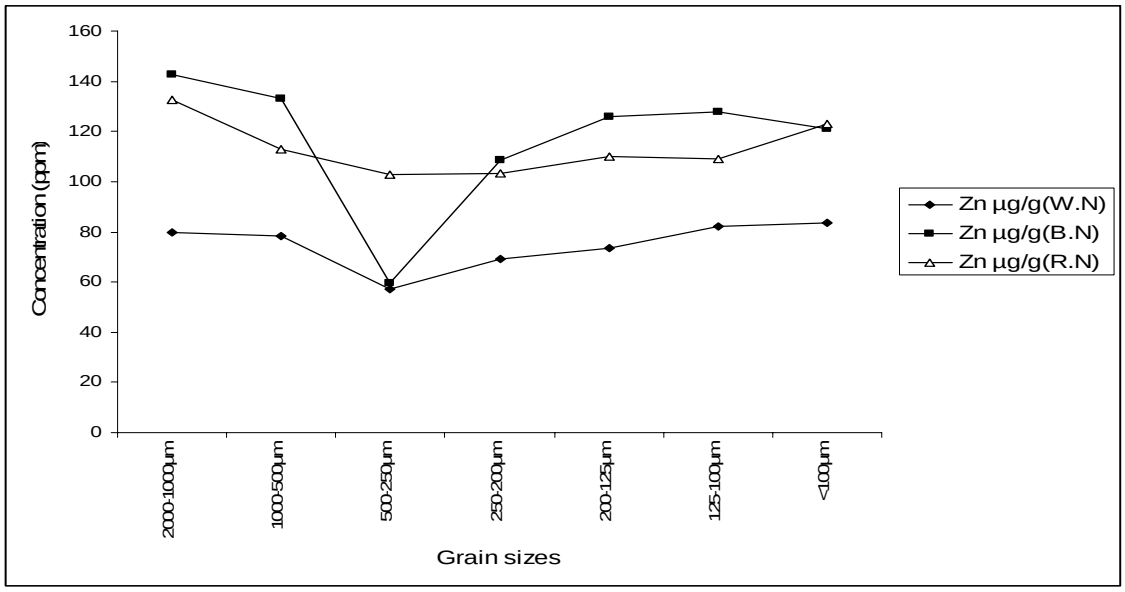

Fig. 4.28: Plot of Zn concentration as a function of sediment grain size in White, Blue and River Nile

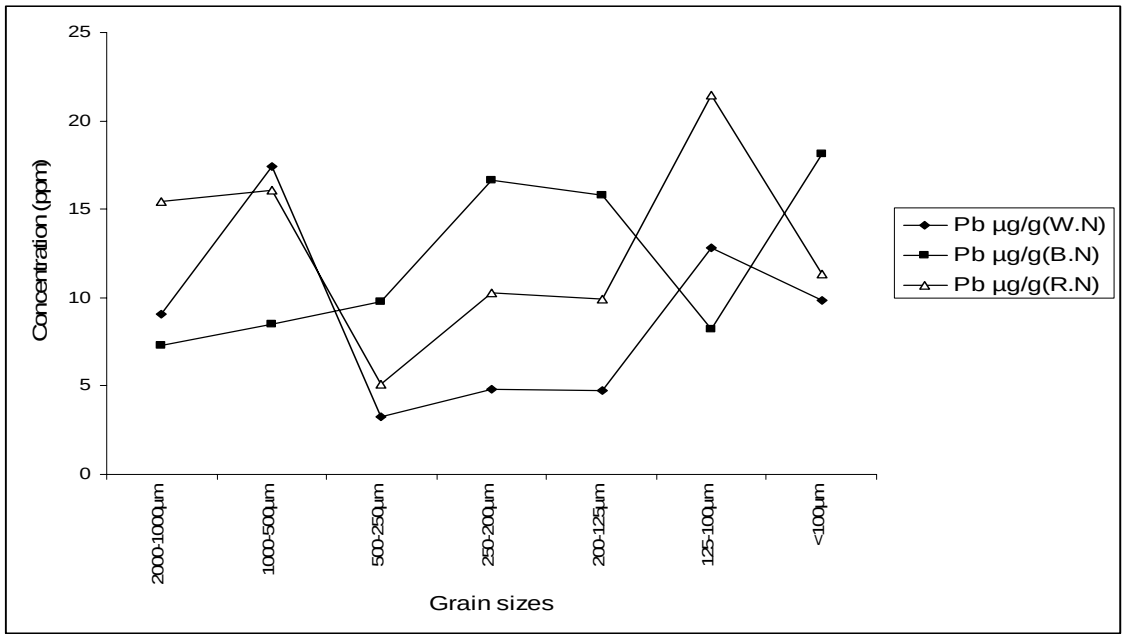

Fig.4.29: Plot of Pb concentration as a function of sediment grain size in White, Blue and River Nile

4.3 Correlation matrices between U-238 and Th-232 and heavy metals contents in sediments

The study of correlation of U-238 and Th-232 as natural radionuclides and heavy metals in sediments from the three sites (Blue, White and River Nile) presented in table (4.5). Positive correlation between all elements was noticed, and from correlation coefficient insignificant correlation was observed for natural radionuclides (^{238}U, ^{232}Th) and heavy metals.

Table 4.5: Correlation coefficient between Natural radionuclides (^{238}U and ^{232}Th) and some heavy metals content in River sediments

	Fe	Ca	Zn	Ni	Cu	Mn	Mg	Pb	U	Th
Fe	1.00									
Ca	**0.65**	1.00								
Zn	**0.98**	**0.57**	1.00							
Ni	**0.60**	**0.59**	**0.59**	1.00						
Cu	**0.89**	**0.53**	**0.90**	**0.60**	1.00					
Mn	**0.76**	**0.67**	**0.80**	**0.64**	**0.74**	1.00				
Mg	0.08	**0.51**	0.03	0.13	0.08	0.13	1.00			
Pb	0.30	0.39	0.29	**0.57**	0.44	0.37	0.18	1.00		
U	0.44	0.21	0.45	0.11	0.40	0.19	0.15	0.32	1.00	
Th	0.49	0.2	**0.52**	0.15	**0.50**	0.30	0.23	0.34	**0.95**	1.00

CONCLUSIONS

From the measurements of activity concentration for ^{238}U, ^{232}Th and ^{40}K in different grain sizes of river surface sediments from White, Blue and River Nile in Khartoum state, the following conclusions can be drown:

The activity concentration for the elements of interest in the bulk sample offer base line data in rivers surface sediments in Khartoum state and from the values obtained the levels of natural and anthropogenic radioactivity are in the similar range of worldwide data.

Activity concentration of natural radionuclides (^{238}U,^{232}Th and ^{40}K) show negative correlation with grain size in the sediments, i.e. activity concentration increases with decreasing particle size, whereas for artificial (^{137}Cs) there no clear behavior with respect to grain size.

The mean activity concentrations of ^{238}U, ^{232}Th and ^{40}K in the three rivers show similar values with exemption of ^{40}K in Blue Nile which show higher value in comparison to other locations.

The scattered of the values within the same fractions appear more pronounced in Blue Nile and River Nile rather than White Nile.

The similar geochemistry of ^{238}U and ^{232}Th reflect their belonging to one group (actinides).

On the other hand, the findings obtained from determination of concentration of selected heavy metals (Mg, Ca, Mn, Fe, Ni, Cu, Zn and Pb) in the same sediments are:

The concentrations of these selected heavy metals show insignificant correlation with grain size except for Fe and to some extend Zn.

The high concentrations of Ca, Mg, Fe and Mn in comparison with other elements indicate crustal origin of these elements in the sediments and confirm the absence of anthropogenic contribution.

The data describe the speciation of selected heavy metals in surface sediments of dynamic system such as the three rivers.

RECOMMENDATION

Further comprehensive seasonal studies based on selected locations along the three rivers can provide a complete image from environmental monitoring point of view.

References

Akram. M, Qureshi .R, M,. Ahmed N, Solaija.T. J (2007): Determination of gamma-emitting radionuclides in the inter-tidal sediments of Balochistan (Pakistan) coast, Arabian Sea. *Radiation Protection Dosimetry*, **123**(2): 286-273.

Akram. M, Qureshi .RM, Ahmed N, Solaija. T. (2006b): Gamma-emitting radionuclides in the shallow Marine sediments of the Sindh Coast, Arabian Sea. *Radiation Protection Dosimetry,* **118**(4): 440-447.

Alamm. N., Chowdhurym. I., Kamalm., Ghose S., Mahmmod N., Matin A. K. M. A., Saikat S. Q. (1997): Radioactivity in sediments of the Karnaphuli River estuary and the Bay of Bengal. *Health phys*ics, **73**(2): 385-387.

Baar, G. E., Lambert, S. J., & Carter, A. (1979): Uranium isotope disequilibrium in ground waters of South-Eastern New Mexico and implications regarding age-dating of waters. *Isotopic Hydrology*, pp: 645, IAEA.

Degens, E.T., Khoo, F., and Michaelis, W. (1977): Uranium anomaly in Black Sea sediments. *Nature*, **269**: 566-569.

Fredrickson, J.K., Zakara, J.M., Kennedy, D.W., Duff, M.C., Gorby, Y.A., Li, M.W., and Krupkak, K.M. (2000): Reduction of U (VI) in goethite (ά –FeOOH) suspensions by a dissimilatory metal–reducing bacteria. *Journal of The Geochemical Society and The Meteoritical Society*, **64**(18): 3085-3098.

Gascoyne, M. (1992): Geochemistry of actinides and their daughters. Cited in *Uranium Series Disequilibrium: Applications to Earth, Marine, and Environmental Sciences* (ed M. Ivanovich and R. S .Harmon), pp. 43-61. Calrendon Press.

Giammar, D. (2001): Geochemistry of uranium at mineral-water interfaces: rates of sorption-desorption and dissolution-precipitation reactions. Ph.D Thesis, California Institute of Technology.

Hakanson L., (1992): Sediment variability. In Burton, J. G.A. (ed.) Sediment Toxicity Assessment, Lewis Publishers, Boca Raton, FL, pp. 19–36.

Henry F. Lamb., C. Richard Bates, Paul V. Coombes., Michael H. Marshall., Mohammed Umer., Sarah J. Davies, and Eshete Dejen. (2007): Late pleistocene desiccation of Lake Tana, source of the Blue Nile. *Quaternary Science Reviews*, 26: 287-299.

Idris, A. M. (1999): Investigation of some heavy metals and radionuclides in sediments from the Sudanese coast Red Sea. M.Sc Thesis, University of Khartoum.

Isinkaye, M. O, Ajayi, I. R (2006): Natural background dose and radium equivalent measurement at Ikogosi warm spring, Nigeria. *Radiation Protection Dosimetry*, 121(4): 466-468.

Ivanovich, M., and Harmon , R.S (1992): Uranium series disequilibrium: *Application to Earth ,Marine, and Environmental Science* (2nd ed), Oxford University Press, New York.

Johansson, T. B., Akselsson, R., and Johansson, S.A.E (1970): *Nuclear Instruments Methods in physics research section*, **84**,141.

John, D; and William, J.M. (1989): Heavy metal concentrations in Ohio River sediments-longitudinal and temporal patterns, *OHIO Journal of Science*, **89**(5): 172-175.

Korede, A.O.I. (2005) Effect of environmental conditions on heavy metal, binding forms. MSc Thesis, UNESCO-IHE, Institute for Water Education, Delft, The Netherlands

Ku, T. L., and Lin, M. C. (1976): Ra-226 Distribution in the Antarctic Ocean. *Earth and planetary Science Letters*, **33**: 236-248.

Ku, T. L., Knauss, K. G., and Mathieu, G. G. (1977): Uranium in open Ocean: concentration and isotopic composition. *Deep-Sea Research*, **24**: 1005–1017.

Langmuir, D. (1978): Uranium solutions–mineral equilibria at low temperature with applications to sedimentary ore deposits. *Journal of The Geochemical Society and The Meteoritical Society*, **42**: 547-569.

Lovely, D., and Philips, E.J.P., (1992): Reduction of uranium by desulfovibrio desulfuricans. *Applied and Environmental Microbiology*, **58(**3): 850-856.

Mance, G., and Yates, J. (1984): Proposed environmental quality standards for list II substance in water: nickle. Tech report: TR211.Water Research Center, Medmenham, UK.

Mann, H., and Fyfe, W.S., (1985): Algal uptake of uranium and some other metals: implications for global geochemistry cycling. *Precambrian Research*, **30**: 337-349.

Mantoura, R.F.C., Dickson, A., Riley, J.P. (1978): The complexation of metals with humic materials in natural waters. *Estuarine Coastal Marine Science*, **6**: 387-408.

Michihiro, K. Sugiyama, H; Kataoka, T.; Yunoki,E. Matsunaga, K.(1987): Estimation on adsorption concentrations of U-238 and Ra-226 in the River-bed soil, *Hoken-Butsuri*, **22**(2): 139-146.

Miyake, Y., Saruhashi, K., and Sugimura, Y. (1973): The isotopic ratio $^{234}U/^{238}U$ in Sea water and It's bearings on the isotopic ratio in River waters, records of Oceanographic.

Moore, W. S. (1981) the thorium isotope content of Ocean water. *Earth and planetary Science Letters*, 53: 419-426.

Murphy, W. M. and Shock, E. L. (1999): Environmental aqueous geochemistry of actinides. In uranium: Mineralogy, Geochemistry, and The Environment, (ed. P. C. Burns and R. Finch). *Mineralogical Society of America*, **38**: 221-254.

Nsouli, B., Darwish, T., Thomas, J. P., Zahraman, K., and Roumie, M. (2004): Ni, Cu, Zn and Pb background values determination in representative Lebanese soil using the thick target PIXE technique. *Nuclear Instrumentation and Methods in Physics Research*, **219-220**: 181-186.

Osman, A.A.A. (2006): Effect of redox potential on heavy metal binding forms in polluted Delft canal sediments, M.Sc Thesis, UNESCO-IHE, Institute for Water Education, Delft, The Netherlands.

Osmaond, J.K. and Cowart, J.B. (1992): Ground water. In *Uranium-Series Disequilibrium: Application to Earth, Marine and Environmental Science* (ed. M Ivanovich and R.S. Harmon), pp.290-333, Charendon Press.

Rickert, D.A., Kennedy, V.C., McKenzie, S.W., and Hines, W.G. (1977): A synoptic survey of trace metals in bottom sediments of the Willamette River, Oregon: *U.S. Geological Survey Circular **715**-F*, pp.27.

Roumie, M., Nsouli, B., Zahraman, K., and Reslan, A. (2004): First accelerator based ion beam analysis facility in Lebanon: development and application. *Nuclear Instrumentation and Methods in Physics Research*, **219-220**: 389-393.

Rudd, T.M.S., and Lester, J.N.(1984): Formation and conditional stability constant of complexes formed between heavy metals and bacterial extracelluar polymers. *Water Research*, **18** : 379.

Saad, H. R, Al-Azmi. D (2002): Radioactivity concentrations in sediments and their correlation to the coastal structure in Kuwait. *Applied Radiation and Isotopes*, **56**(6): 991-997.

Saenz, V., Blasco, J., and Abelard, G., (2003): Speciation of heavy metals in recent sediments of three coastal ecosystems in the Gulf of Cadiz, Southwest Iberian Peninsula. *Environmental Toxicology and Chemistry*, **22**(12): 2833-2839.

Salomons, W. and Förstner, U. (1984): Metals in the hydrocycle. Springer, Berlin.

Sam, A. K., Ahmed, M. M.O., El khangi, F.A., El Nigumi, Y.O. (2000a): Uranium and thorium isotopes in some Red Sea sediments. *International Journal for chemical aspects of Nuclear Science and Technology*, **88**: 307-312.

Sam, A.K., ElGanawi, A.A.., Ahmed, M.M.A., El khangi, F.A., (1998a): Distrtibution of some natural and anthropogenic radionuclides in Sudanese harbour sediments. *Journal of Radioanlytical and Nuclear Chemistry*, **237**(1-2): 103-107.

Sam, A. K., Ahmed, M. M.O., El khangi, F.A., El Nigumi, Y.O., and Elis, H. (1998b): Radioactivity levels in the Red Sea coastal environment of Sudan. *Marine Pollution Bulletin*, **36**(1): 19-26.

Sam, A. K., Ahmed, (1998) Radiochemical studies on environmental radioactivity in Sudan, Ph. D Thesis, University of Khartoum.

Shawky, S., Amer, H., Nada, A.A., El-Maksoud, T.M.A., Ibrahiem, N. M. (2001): Characteristics of NORM in the oil industry from Eastern and Western deserts of Egypt. *Applied Radiation and Isotopes*, **55:** 135-139.

Singh A. K., Hasnain S. I., and Banerjee, D. K. (1999): Grain size and geochemical partitioning of heavy metals in sediments of the Damodar River: A tributary of the Lower Ganga, India. *Journal of Environmental geology*, **39**(1): 90-98.

Sir El Khatim, D.A. (2002): Determination of radionuclides and trace elements in Marine sediments and biota from the Red Sea coast, M.Sc Thesis, University of Khartoum.

Skwarzec, B., A. Boryło, D. Strumin´ska (2002) U-234 and U-238 isotopes in water and sediments of the Southern Baltic. *Journal of Environmental Radioactivity*, 61:345–363.

Suzuki, Y. and Banfield, J. (1999): Geomicrobiology of uranium. In: Uranium: Mineralogy, Geochemistry, and the Environment, (ed. P. C. Burns and R. Finch). *Mineralogical Society of America*, **38**: 393-432.

Uosif, M. A. M (2007) Gamma-ray spectroscopic analysis of selected samples from Nile River sediments in Upper Egypt. *Radiation Protection Dosimetry*, 123(2): 215-220.

UNSCEAR (2000a)—United Nations Scientific Committee on the Effects of Atomic Radiation. Sources and Effects of Ionizing Radiation, vol. I. New York: United Nations; pp. 123.

UNSCEAR (2000b)—United Nations Scientific Committee on the Effects of Atomic Radiation. Sources and Effects of Ionizing Radiation, vol. II. New York: United Nations; pp. 346.

UNSCEAR (1993): United Nation Scientific Committee on the Effect of Atomic Radiation, Report. United Nations, New York.

Van Aardt, W.j. and Erdmann, R. (2004): Heavy metals (Cd, Pb, Cu, Zn) in the mudfish sediments from three hard-water dams of the Mooi River catchments, South Africa. *Water SA*, **30**(2): 211-218.

Wilber, W.G., and Hunter, J.V. (1979): The impact of urbanization on the distribution of heavy metals in bottom sediments of the Saddle River. *Water Resources Bulletin*, **15**(3): 790-800.

Yuanxum, Z; Lin, E; Li, D; Wang, Y; Yu, Y; Wang, C; Shen, W; Zhi, M; Zhang, G; Li, Y (2003): PIXE and radioactivity measurement for elemental determination in River water and sediment samples. *Journal of radioanalytical and nuclear chemistry*, **258** (2): 415-419.

Zielinski, R.A., Otton, J.K. , Vanty, R.B., and Pierson, C.T.(1988): The aqueous geochemistry of uranium in drainage containing uraniferous organic rich sediments, Lake of Tahoe , Nevada , U.S.A. *uranium*, **4**: 281- 305.

Table (4.6): Activity concentration (Bq kg^{-1}) of U-238, Th-232, K-40 and Cs-137 in different fractions of Blue Nile sediments

Code	U-238	Th-232	K-40	Cs-137	Size(µm)
B-1.1	15.99	18.13	402.99	1.79	2000
B-1.2	16.44	16.62	367.69	1.87	2000
B-1.3	17.84	16.33	396.51	4.76	2000
B-1.4	20.08	17.07	432.62	5.11	2000
B-2.1	21.57	21.59	509.36	1.65	1000
B-2.2	21.12	21.82	483.84	5.04	1000
B-2.3	21.69	19.28	538.68	5.12	1000
B-2.4	16.67	18.33	462.18	5.00	1000
B-3.1	16.78	14.10	501.54	2.14	500
B-3.2	17.55	14.63	424.52	3.07	500
B-3.3	13.01	8.94	547.14	0.71	500
B-3.4	11.68	7.00	517.91	1.09	500
B-4.1	19.12	18.73	624.15	3.67	250
B-4.2	18.11	14.71	606.89	3.33	250
B-4.3	17.12	19.52	619.41	6.98	250
B-4.4	16.03	17.45	608.12	3.23	250
B-5.1	14.03	11.82	293.93	1.80	200
B-5.2	22.63	17.93	382.42	3.44	200
B-5.3	20.44	17.99	392.31	3.40	200
B-5.4	8.84	8.18	209.77	2.11	200
B-6.1	22.78	18.77	605.77	3.72	125
B-6.2	22.64	19.68	608.39	4.77	125
B-6.3	21.32	19.29	610.68	4.84	125
B-6.4	19.88	20.36	571.90	5.65	125
B-7.1	28.13	26.22	523.90	2.80	100
B-7.2	29.11	23.38	529.79	4.86	100
B-7.3	28.66	24.64	545.96	4.56	100
B-7.4	28.46	23.73	523.86	4.32	100
MB1	16.70	16.63	426.76	3.80	
MB2	13.73	15.59	419.16	1.93	
MB3	14.75	14.68	398.48	3.06	
MB4	14.95	16.125	447.85	2.88	

Table (4.7): Activity concentration (Bq kg^{-1}) of U-238, Th-232, K-40 and Cs-137 in different fractions of White Nile sediments

Code	U-238	Th-232	K-40	Cs-137	Size(µm)
W-1.1	19.68	16.89	361.44	0.30	2000
W-1.2	13.88	11.44	220.36	ND	2000
W-1.3	13.88	11.36	220.36	ND	2000
W-1.4	19.96	17.38	364.93	0.34	2000
W-2.1	5.93	6.17	154.48	ND	1000
W-2.2	13.32	12.58	280.14	0.48	1000
W-2.3	16.18	14.64	302.30	0.65	1000
W-2.4	17.20	14.13	296.35	ND	1000
W-3.1	13.22	10.95	296.22	0.41	500
W-3.2	13.23	11.32	297.40	ND	500
W-3.3	12.36	11.98	282.09	ND	500
W-3.4	11.99	10.09	268.91	0.45	500
W-4.1	15.41	13.79	366.18	0.56	250
W-4.2	16.37	14.02	391.86	ND	250
W-4.3	14.44	14.28	441.13	0.36	250
W-4.4	15.60	13.14	383.13	ND	250
W-5.1	17.95	16.31	462.94	ND	200
W-5.2	18.06	17.52	418.39	ND	200
W-5.3	18.78	16.52	489.23	0.59	200
W-5.4	19.15	17.51	465.05	ND	200
W-6.1	24.81	22.27	582.58	ND	125
W-6.2	21.29	22.26	353.31	ND	125
W-6.3	21.90	21.62	508.20	2.76	125
W-6.4	20.58	18.01	443.79	2.88	125
W-7.1	26.39	25.50	460.82	ND	100
W-7.2	25.87	27.22	473.85	ND	100
W-7.3	24.94	24.16	500.10	ND	100
W-7.4	29.10	25.75	549.52	ND	100
MW1	17.39	16.93	425.19	0.63	
MW2	15.59	17.49	404.25	0.49	
MW3	16.95	17.69	430.51	ND	
MW4	16.21	16.52	392.31	ND	

Table (4.8): Activity concentration (Bq kg^{-1}) of U-238, Th-232, K-40 and Cs-137 in different fractions of River Nile sediments

Code	U-238	Th-232	K-40	Cs-137	Size(µm)
R-1.1	19.44	18.78	401.23	4.26	2000
R-1.2	20.35	18.68	385.81	3.94	2000
R-1.3	18.22	18.23	388.29	3.28	2000
R-1.4	20.39	18.88	404.89	5.60	2000
R-2.1	17.76	16.93	316.10	2.95	1000
R-2.2	17.47	14.76	336.90	3.54	1000
R-2.3	16.63	16.67	326.11	3.77	1000
R-2.4	16.60	12.95	318.39	3.13	1000
R-3.1	15.24	15.68	357.59	2.48	500
R-3.2	14.84	14.12	314.07	3.01	500
R-3.3	16.28	14.25	319.10	2.83	500
R-3.4	15.35	12.60	302.13	2.58	0.5
R-4.1	17.78	18.24	474.31	2.28	250
R-4.2	23.37	22.37	692.79	ND	250
R-4.3	14.21	13.14	300.41	1.73	250
R-4.4	18.27	16.20	432.82	2.60	250
R-5.1	19.73	15.02	363.43	2.12	200
R-5.2	23.30	18.02	381.96	2.46	200
R-5.3	23.30	18.02	381.96	2.46	200
R-5.4	24.29	21.43	292.43	3.32	200
R-6.1	22.29	18.34	367.66	2.80	125
R-6.2	21.91	22.80	407.81	2.94	125
R-6.3	21.85	21.53	508.20	2.76	125
R-6.4	20.68	18.08	442.04	2.82	125
R-7.2	20.15	18.42	430.63	2.91	100
R-7.3	20.92	19.25	425.54	3.14	100
R-7.4	19.95	18.77	444.04	2.76	100
MR1	15.74	17.45	425.19	0.63	
MR2	16.39	18.57	404.25	0.49	
MR3	16.32	18.92	430.51	ND	
MR4	16.10	15.53	392.31	ND	

Table (4.9): Concentration (mg/g or µg/g) dry weight of heavy metals in different fractions of White Nile sediments

Code	Fe mg/g	Ca mg/g	Zn µg/g	Ni µg/g	Cu µg/g	Mn mg/g	Mg mg/g	Pb µg/g
W-1.1	60.46	51.50	82.09	51.12	34.05	1.78	17.00	5.51
W-1.2	65.19	43.45	77.77	37.13	36.71	1.64	18.49	12.62
W-2.1	55.40	36.50	78.90	23.2	41.28	1.24	16.49	23.08
W-2.2	56.82	38.75	77.29	65.9	35.86	1.65	15.63	11.78
W-3.1	37.80	24.31	56.70	28.09	21.52	0.83	12.22	ND
W-3.2	41.76	27.01	57.82	12.77	31.21	0.92	13.77	6.534
W-4.1	48.03	23.28	68.05	54.02	20.59	0.87	12.24	4.96
W-4.2	50.27	22.89	69.88	22.6	17.61	1.03	11.32	4.74
W-5.1	50.60	50.60	69.07	17.41	33.65	0.89	12.06	6.359
W-5.2	51.82	51.82	78.26	38.94	16.30	0.86	12.54	3.09
W-6.1	61.31	29.22	77.53	35.95	29.03	1.36	14.62	9.708
W-6.2	62.15	30.10	86.41	44.43	43.39	1.33	14.82	15.86
W-7.1	67.31	28.62	91.98	36.64	44.09	1.31	14.48	5.17
W-7.2	60.26	29.12	74.75	25.49	54.81	0.99	13.13	14.48
MW1	54.43	26.49	75.31	51.84	45.63	1.23	13.45	ND
MW2	60.67	25.62	79.52	45.08	32.50	1.13	13.27	5.52

Table (4.10): Concentration in (mg/g or µg/g) dry weight of heavy metals in different fractions of Blue Nile sediments

Code	Fe mg/g	Ca) mg/g	Zn µg/g	Ni µg/g	Cu µg/g	Mn mg/g	Mg mg/g	Pb µg/g
B-1.1	101.44	41.12	134.80	69.84	70.19	1.91	13.73	13.08
B-1.2	103.39	37.96	150.60	53.47	90.78	1.73	13.80	1.49
B-2.1	98.08	35.91	133.10	34.90	69.27	1.91	14.40	0.94
B-2.2	100.99	38.12	133.00	40.94	79.30	1.84	11.99	16.10
B-3.1	39.99	24.36	49.66	14.31	26.41	1.74	89.24	7.66
B-3.2	58.93	29.33	69.41	38.94	22.73	9.22	74.62	11.83
B-4.1	82.53	35.44	103.20	25.68	54.81	1.43	12.81	14.37
B-4.2	87.64	35.15	114.10	54.13	65.93	1.66	12.44	18.86
B-5.1	96.46	38.51	121.00	80.57	60.02	1.60	12.44	18.19
B-5.2	106.34	38.32	130.70	84.07	65.92	1.54	13.79	13.46
B-6.1	96.68	37.50	126.40	26.85	39.49	1.57	11.48	8.82
B-6.2	100.01	33.36	128.80	57.62	64.81	1.58	12.58	7.5
B-7.1	94.96	37.78	115.60	63.71	73.51	1.66	12.58	16.62
B-7.2	99.34	38.56	126.90	44.89	76.25	1.64	12.92	19.67
MB1	90.05	38.87	130.90	72.37	76.72	1.63	13.76	13.88
MB2	89.77	42.03	130.80	69.14	73.89	1.59	13.65	ND

Table (4.11): Concentration in (mg/g or µg/g) dry weight of heavy metals in different fractions of River Nile sediments

Code	Fe mg/g	Ca mg/g	Zn µg/g	Ni µg/g	Cu µg/g	Mn mg/g	Mg mg/g	Pb µg/g
R-1.1	96.32	32.18	128.30	37.93	68.66	1.73	11.64	8.80
R-1.2	96.02	33.01	136.90	75.26	66.16	1.84	12.42	22.06
R-2.1	87.84	29.95	118.80	60.58	64.93	1.87	11.97	19.59
R-2.2	83.44	29.64	106.70	41.98	55.85	1.83	10.68	12.54
R-3.1	78.88	29.54	107.80	46.97	59.75	1.58	11.62	1.28
R-3.2	77.32	28.16	97.59	28.82	49.85	1.66	10.91	8.93
R-4.1	86.82	42.02	102.10	65.62	60.93	1.61	12.36	11.30
R-4.2	82.57	30.76	104.50	56.04	38.71	1.46	12.16	9.27
R-5.1	92.50	38.40	124.90	45.34	59.18	1.44	12.48	5.55
R-5.2	81.02	40.45	94.87	23.95	45.62	1.28	12.20	14.27
R-6.1	87.82	36.57	112.00	76.19	74.59	1.47	12.76	21.48
R-6.2	84.49	31.27	105.80	39.17	57.92	1.42	12.79	21.48
R-7.1	98.00	34.67	119.20	31.52	68.36	1.62	12.20	17.95
R-7.2	97.82	35.20	127.10	53.59	65.59	1.73	11.82	4.65
MR1	90.28	37.19	115.10	44.42	41.93	1.61	12.21	10.28
MR2	90.73	32.97	114.90	42.93	54.39	1.66	11.89	26.42